Journal of Medicinal Chemistry

Perspective

pubs.acs.org/jmc

Blocking Blood Flow to Solid Tumors by Destabilizing Tubulin: An Approach to Targeting Tumor Growth

María-Jesús Pérez-Pérez,*[,#] Eva-María Priego,[#] Oskía Bueno,[#] Maria Solange Martins,[†] María-Dolores Canela,[#] and Sandra Liekens[†]

[#]Instituto de Química Médica (IQM-CSIC), Juan de la Cierva 3, E-28006 Madrid, Spain

[†]Rega Institute for Medical Research, KU Leuven, B-3000 Leuven, Belgium

ABSTRACT: The unique characteristics of the tumor vasculature offer the possibility to selectively target tumor growth and vascularization using tubulin-destabilizing agents. Evidence accumulated with combretastatin A-4 (CA-4) and its prodrug CA-4P support the therapeutic value of compounds sharing this mechanism of action. However, the chemical instability and poor solubility of CA-4 demand alternative compounds that are able to surmount these limitations. This Perspective illustrates the different classes of compounds that behave similar to CA-4, analyzes their binding mode to $\alpha\beta$-tubulin according to recently available structural complexes, and includes described approaches to improve their delivery. In addition, dissecting the mechanism of action of CA-4 and analogues allows a closer insight into the advantages and drawbacks associated with these tubulin-destabilizing agents that behave as vascular disrupting agents (VDAs).

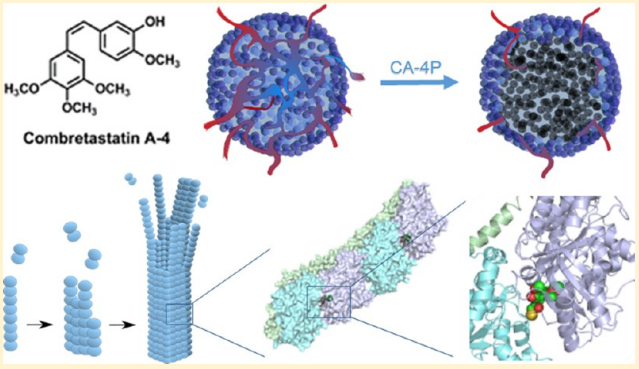

1. TUMOR VASCULARIZATION

The requirement of vascularization for tumor growth and metastasis has become one of the greatest areas of research in recent years. It is widely accepted that a solid tumor cannot grow further than approximately 2 mm^3 without blood vessels that provide oxygen and nutrients. Two main approaches have been followed to target tumor vascularization: inhibition of angiogenesis, that is, the formation of new blood vessels, or targeting the already existing vasculature.[1] Both approaches are directed against endothelial cells, a cell type that is genetically more stable and less prone to mutations compared to tumor cells.[2−4]

Angiogenesis has been extensively investigated promoting fundamental work on how this process occurs under physiological and pathological conditions.[5] There are currently a number of approved drugs, both monoclonal antibodies and small molecules, that are able to affect this process.[6] However, from an anticancer perspective, antiangiogenic agents have not accomplished their expectations. Clinical data indicate that treatment with these agents is accompanied by lack of efficacy, resistance development, and toxicity.[7] Still, antiangiogenic agents have proven useful in combination therapies, and applications outside cancer treatment continue to be explored.[7]

The second approach targeting the tumor vasculature relies on the so-called vascular-disrupting agents, commonly designated as VDAs.[1] These agents target already existing vessels in the tumor environment, thereby provoking a rapid collapse of the tumor vasculature leading to necrosis at the tumor core. Although it is not always easy to dissect between an antiangiogenic and a VDA effect, antiangiogenic agents are considered to be cytostatic against endothelial cells and are particularly active at early stage (small) tumors. These compounds should ideally be administered for long periods, so almost chronically. On the other hand, VDAs are cytotoxic and exert an almost immediate effect on the existing tumor vessels leading to a rapid vascular collapse and subsequent tumor cell death. Therefore, they are particularly efficient against large tumors and should be administered acutely.[8]

2. VASCULAR DISRUPTING AGENTS (VDAS)

2.1. Characteristics of the Tumor Vasculature. Vascular endothelial cells are planar cells that cover the internal/luminal surface of blood vessels, thus ensuring laminar blood flow and providing a nonthrombogenic surface. Endothelial cells are highly heterogeneous and display different morphologies and functions depending on their location (e.g., liver versus lung, macro- versus microvasculature). Moreover, significant differences exist between physiological vessels and vessels in the tumor microenvironment.[9] The normal vasculature is a well-organized network that is strictly controlled by a balance between proangiogenic and antiangiogenic factors and is arranged in a hierarchy of well-differentiated arteries, arterioles, capillaries, venules, and veins. In contrast, the overexpression of proangiogenic factors in the tumor environment results in an unevenly distributed and chaotic vasculature with irregular

Received: March 29, 2016
Published: June 27, 2016

DOI: 10.1021/acs.jmedchem.6b00463
J. Med. Chem. 2016, 59, 8685−8711

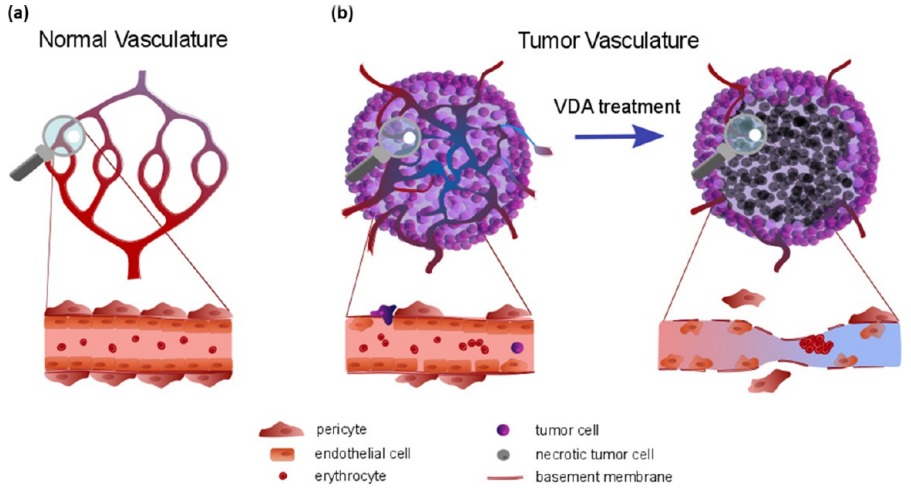

Figure 1. Schematic representation of the effects of VDA treatment on tumor vascularization. (a) In the normal vasculature, blood vessels are organized hierarchically and the basement membrane and pericytes provide structure and stability to the vessels. (b) Intratumoral vessels are chaotic and often lack pericytes and a proper basement membrane. Reduced blood flow renders the tumor center hypoxic, and tumor cells can invade the unstable and leaky vessels. VDA treatment results in disruption of the cytoskeleton and reduced cell−cell junctions, further increasing vascular leakage. This triggers a cascade of events, resulting in a reduction of blood flow, vessel occlusion, and necrosis in the tumor center. In the periphery, there is a rim of surviving tumor cells that receive nutritional support from nearby blood vessels, which are less responsive to VDAs.

branches and the formation of arteriovenous shunts. Moreover, tumor blood vessels are structurally abnormal and often lack pericytes and a proper basement membrane, which makes these vessels more fragile and immature (Figure 1).[8] These morphological abnormalities have a significant impact on vessel function, i.e., blood vessel permeability is increased in the tumor, leading to extravasation of macromolecules and increased interstitial pressure. Vascular resistance is equally increased in tumor vessels, and blood flow is reduced. Thus, any alteration of blood vessel perfusion that would not be relevant for a normal vessel may be catastrophic for the intratumoral vasculature,[2] leading to ischemia and tumor cell death (Figure 1). Agents that may lead to such vascular destruction were designated as VDAs.[1] It should be noted that imaging techniques provide evidence that the vascular damage after VDA treatment is confined to the tumor vessel network.[8] It is also relevant to mention that cells at the outer rim of the tumor are not affected by the VDAs, probably due to nutritional support from the nearby blood vessels which are less responsive to VDAs.[10]

2.2. Classification of VDAs. Early reviews on VDAs a decade ago proposed a classification of these agents in two main groups:[11] ligand-directed VDAs and small molecules (Figure 2a). The ligand-directed VDAs make use of antibodies, peptides, or growth factors to target toxins or procoagulants to the tumor endothelium.[12] The second class of VDAs contains small molecules and has been further classified into derivatives of 8-flavon acetic acid (**1**, FAA, Figure 2a), designated as flavonoids in previous reviews,[12] and tubulin-depolymerizing agents. According to IUPAC recommendations, the flavonoid designation, currently under evaluation, is too wide and includes among others, flavones, isoflavones, neoflavones, chalcones, dehydrochalcones, aurones, etc. As we will later describe, compounds belonging to these structural families (i.e., chalcones) are tubulin-depolymerizing agents, so the designation of flavone derivatives for this first group should be more accurate than flavonoids, and we propose such designation.

FAA and its best studied derivative 5,6-dimethylxanthenone-4-acetic acid (**2**, DMXAA, ASA404, Figure 2a)[12] induce the activation of nuclear factor κB (NF-κB) which increases the production of various cytokines, including tumor necrosis factor-α (TNF-α). As a consequence endothelial cells enter apoptosis, leading to hemorrhagic necrosis of the tumor. Compound **2** was discontinued after phase III clinical trials against advanced NSCLC.[13,14] More details about the biological activity of FAA and DMXAA can be found in a very recent review.[15]

The second group of small molecules that behave as VDAs has been designated as tubulin-depolymerizing VDAs,[8] and they will be the subject of this Perspective. This group comprises a very large and structurally diverse group of compounds that bind at the colchicine site in tubulin.

2.3. VDAs Acting at Tubulin. Microtubules are dynamic structures that, together with actin microfilaments and intermediate filaments, constitute the cellular cytoskeleton. Besides their well-known role in cell division, their functions involve maintenance of cell shape and morphology, cellular motility, and trafficking of organelles and vesicles.[16] Microtubules are formed by the polymerization of heterodimers of α and β tubulin. These heterodimers assemble head to tail into linear protofilaments, which further polymerize in a polar manner to form the microtubules that have a plus end where β-tubulin is exposed and a minus end where the α-subunit is present (Figure 2b). Binding and hydrolysis of GTP at the microtubule ends is directly involved in microtubule dynamics.[16]

Colchicine (**3**) (Figure 2a) is a natural alkaloid present in different species particularly in *Colchicum autumnale*. In 1968, this alkaloid was used for the identification of tubulin, a protein unknown until then.[17] Colchicine was characterized as a potent cytotoxic agent that binds tubulin at the αβ-tubulin interface[18] and causes microtubule depolymerization,[19] probably by inhibiting assembly of the protofilaments. However, due to a very narrow therapeutic window, colchicine has been discarded as an antitumor drug, although at lower doses it is used for the treatment of gout, familiar Mediterranean fever, osteoarthritis, pericarditis, and atherosclerosis.[20]

DOI: 10.1021/acs.jmedchem.6b00463
J. Med. Chem. 2016, 59, 8685−8711

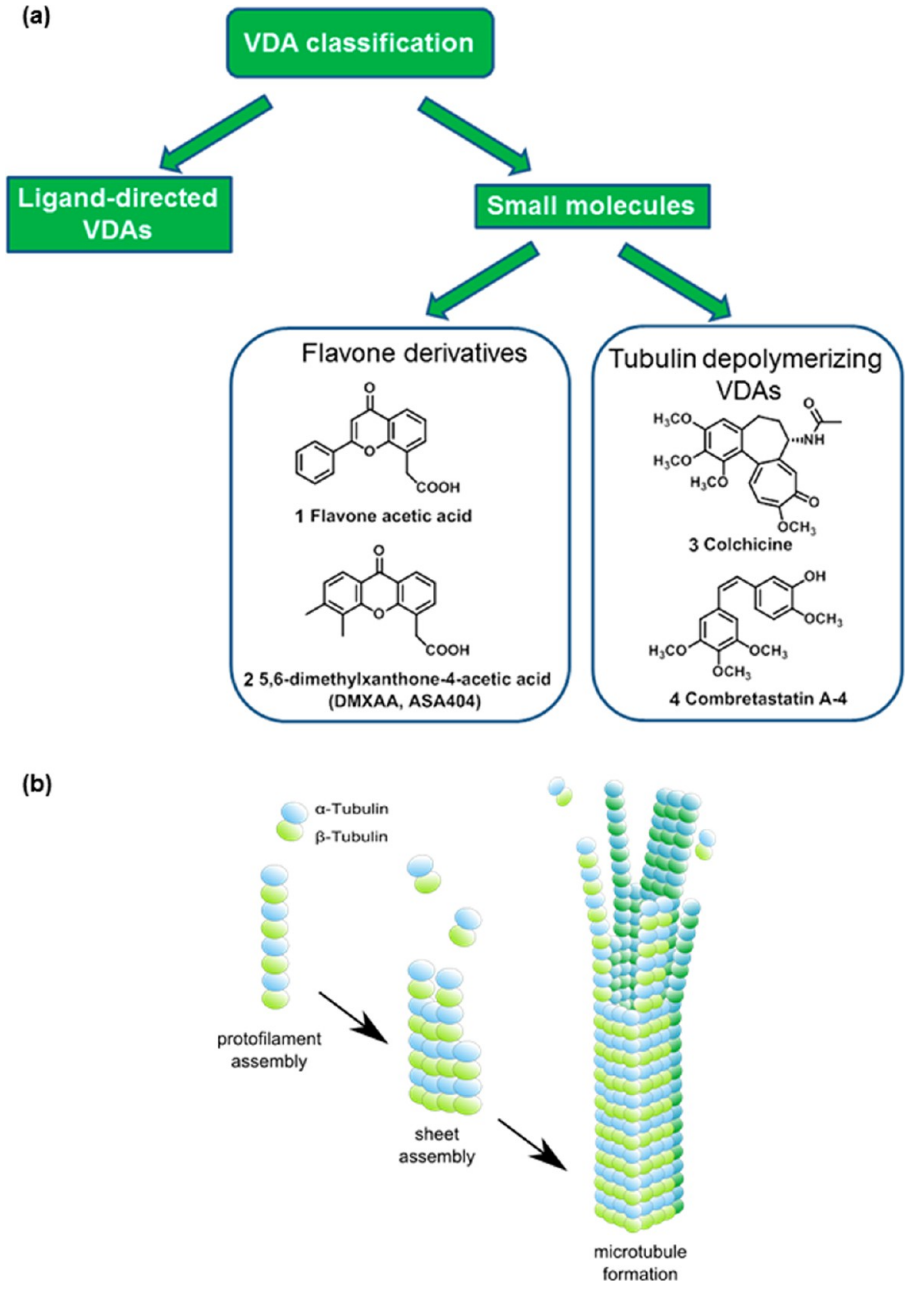

Figure 2. (a) Classification of VDAs. (b) Incorporation of $\alpha\beta$-tubulin dimers into protofilaments, sheet assembly, and microtubule formation.

The prototype compound among VDAs acting at the colchicine site in tubulin is combretastatin A-4 (**4**, CA-4) (Figure 2a), a natural product isolated from *Combretum caffum*.[21] Binding of CA-4 to the colchicine site was established early through a competitive-binding assay.[22] Additional studies demonstrated rapid binding of CA-4 to tubulin in contrast to the relatively slow and temperature-dependent binding of colchicine. Moreover, dissociation of CA-4 from tubulin in the presence of high concentrations of radiolabeled colchicine was quite rapid, indicating a different kinetic behavior in tubulin binding between CA-4 and colchicine.[23] CA-4 was the first compound reported to show vascular disrupting properties at a tolerated dose.[24] Although identified more than two decades ago, the mechanism of action of CA-4 is still not fully elucidated. It is known that the binding of CA-4 to tubulin at the colchicine site inhibits tubulin polymerization, leading to the activation of RhoA, a protein that is crucial for coordinating the interactions of F-actin and microtubules in the cytoskeleton,[3] as will later be discussed in section 5.1.1.

In addition, CA-4, as a colchicine site binder, has antimitotic activity in rapidly proliferating cells by interfering with mitotic spindle formation and chromosome alignment (see section 5.2.1). Compared to microtubule targeting agents acting at other tubulin sites (i.e., taxol and vinca alkaloids) for which drug resistance is an important issue due to P-glycoprotein (P-gp) or βIII-tubulin overexpression, compounds binding at the colchicine site retain activity against cell lines that overexpress these factors.[25]

The potential therapeutic value of vascular disrupting agents binding at the colchicine site has led to a plethora of original and review articles on this subject in recent years. We have made an effort to refer to these review articles throughout this

DOI: 10.1021/acs.jmedchem.6b00463
J. Med. Chem. 2016, 59, 8685−8711

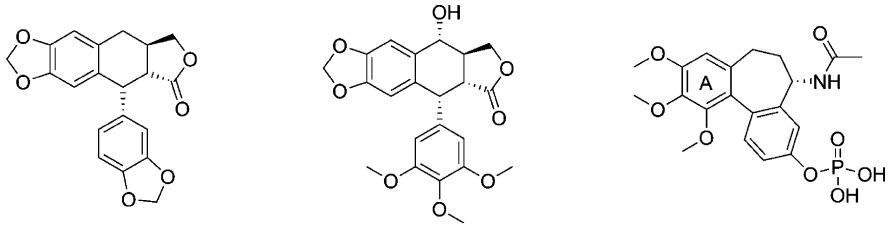

5 Polygamain 6 Podophyllotoxin 7 ZD6126

Figure 3. Examples of natural products binding tubulin at the colchicine site (**5**, **6**) and a colchicine derivative tested in clinical trials (**7**).

Perspective, while it has not been our intention to cover exhaustively the information that can be found in such articles. Our review is centered on combretastatin A-4 and how medicinal chemistry approaches have tried to improve the limitations of this archetypical VDA (particularly instability and poor solubility). We have also included compounds whose structure differs from CA-4 but that have provided significant VDA properties, most of them reaching clinical trials. Because solubility and delivery have been a significant limitation for CA-4, a brief reference to prodrugs and other approaches meant to improve the delivery of CA-4 has also been included. Lately, an increasing number of structures of VDA−tubulin complexes have been solved. A section will be devoted to this structural information because it may inspire a new generation of VDAs. It is also very relevant for the future of this family of therapeutic agents to dissect the biological actions of CA-4 because this may pave the way for new interventions. Results obtained from preclinical and clinical studies have been recently reviewed by other authors, and the reader is referred to them.[15,26−28]

As we will discuss later, the biological actions of CA-4 have been investigated in endothelial and tumor cells including effects on the cell cycle and on cell morphology as well as binding to tubulin. Various assays have been established to investigate these CA-4-mediated effects and to demonstrate the combretastatin-like behavior of most of the compounds included in this Perspective. We will briefly mention these assays here. For more detailed information, we refer to the review of Barbier et al.[29] on the molecular mechanisms of antitubulin plant-derived drugs.

In general, VDAs and, in particular, CA-4-like compounds, are submitted to a proliferation assay using tumor (and endothelial) cell lines. CA-4 and analogues are antimitotic, blocking cell cycle progression during mitosis, which can be evidenced by flow cytometry as an increase of cells in G2/M phase. Additionally, mitotically arrested cells may undergo apoptosis, noticed by an increase in the subG1 population (see section 5.2 for pathways involved). To visualize the tubulin-binding effects of the compounds, mitotic spindle organization is investigated by immunofluorescence staining of the cells with an antibody against tubulin. A direct interaction of the compound with tubulin may be shown by measuring tubulin polymerization or by biophysical assays to determine the stoichiometry and the association constant (K_a) including fluorescence spectroscopy using established ligands or radio-ligand displacement using [^{3}H]colchicine. It is interesting to mention that the particularities of tubulin and its associated proteins (microtubule-associated proteins, MAPs) limit the employment of some standard techniques such as surface plasmon resonance (SPR) or ITC to determine kinetics or binding affinity for a small ligand. For example, the tendency of tubulin to self-aggregate makes a biophysical method such as SPR not ideal for these determinations. On the other hand, ITC has mostly been used to characterize the binding of tubulin to MAPs such as stathmin[30] with just a few examples for small ligands.

An additional and convenient assay to show that the compound binds specifically at the colchicine binding site of tubulin is a recently described competition assay with *N*,*N*′-ethylene-bis(iodoacetamide) (EBI)[31] in human breast cancer MDA-MB-231 cells. EBI is an alkylating agent that specifically binds to two cysteine residues present in the colchicine-binding site of tubulin, Cys239 and Cys354. This β-tubulin adduct can be detected by Western blot as a second immunoreactive β-tubulin band that migrates faster than β-tubulin itself. A compound binding at this site will prevent the formation of the β-tubulin adduct.[32,33]

Finally, the capacity to destroy a preexisting vasculature network formed by endothelial cells on Matrigel, a solubilized basement membrane that promotes tube formation, provides evidence for the vascular-disrupting activity of the compound. This should however be confirmed in vivo by imaging of blood flow or vascular shutdown in tumor xenografts.

For most VDAs binding at the colchicine site in tubulin, including CA-4, inhibition of tubulin assembly was found at μM concentrations while cytoxicity in cell culture assays was detected at nM or even sub-nM concentrations. As recently discussed,[34] the reason for this apparent inconsistency is not completely clear, but there are several factors that may contribute to explain this experimental fact. One factor could be that the stoichiometry (compound versus tubulin concentration) required in the tubulin (cell-free) assay to achieve an IC_{50} value might be completely different from the stoichiometry that exists when inhibiting tubulin in cell culture. It is also possible that tubulin depolymerization in cells may release other factors involved in signal transduction so that the biological effect is amplified. In addition, there may be factors directly linked to the limitations and sensitivity of the protein assay.[34]

2.4. Classes of Compounds. A huge number of compounds mimicking combretastatin A-4 have been reported in recent years, most of which have been covered in excellent review articles. A Mini-Perspective article has appeared in this journal in 2006 by Tron et al. covering the medicinal chemistry of combretastatin A-4.[35] A very detailed overview of tubulin inhibitors binding at the colchicine site was published by Miller and collaborators, covering compounds reported up to 2010.[36] Combretastatin A-4 derivatives have also been reviewed by Shan et al.,[37] Marrelli et al.,[38] and very recently by Patil et al.[39] A review focusing on *cis*-restricted isomers has been published by Rajak et al.[40] For those particularly interested in the synthetic pathways applied to obtain these compounds, relevant information can be obtained in the review article of Kaur et al.[41]

DOI: 10.1021/acs.jmedchem.6b00463
J. Med. Chem. 2016, 59, 8685−8711

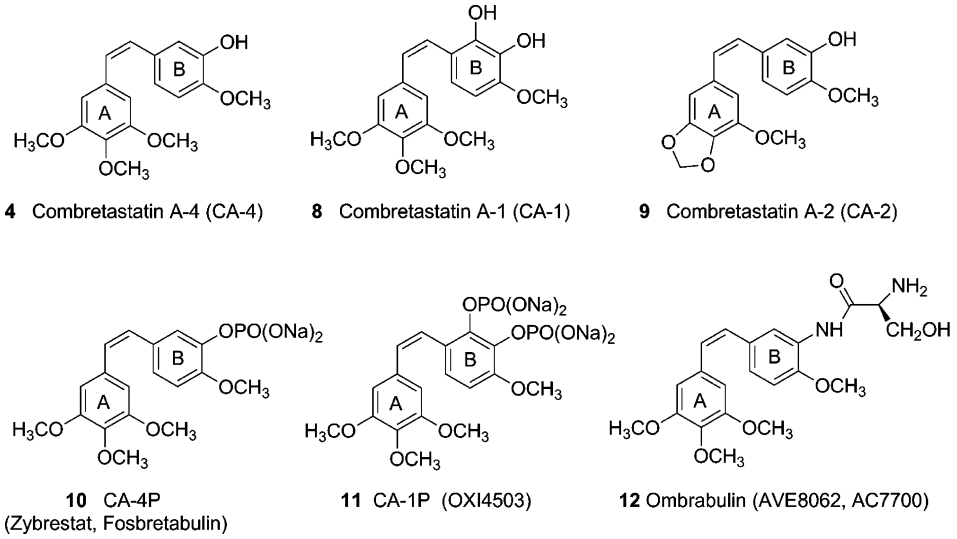

Figure 4. Relevant combretastatins and their prodrugs.

Other authors have performed a classification of the compounds based on structural and docking studies, as the exhaustive review of Alvarez et al.[42] An overview of the role played by computational approaches in the context of the colchicine-binding domain has also been recently reported by Massarotti et al.[43]

In our survey through the different families of compounds that behave as VDAs, we have centered our attention on those compounds that are active in the nM range in cell culture and/or for which animal experiments have been conducted as proof of concept of their VDA capacity. However, no comparison between data coming from different laboratories has been performed.

2.4.1. Combretastatin and Analogues. Before introducing combretastatin A-4 and other combretastatins, it should be mentioned that there are a significant number of natural products whose structure resembles that of colchicine and for which binding at the colchicine site in tubulin and a combretastatin-like behavior has been proven. These include polygamain (**5**)[44] or podophyllotoxin (**6**)[45] as relevant examples (Figure 3). Among colchicine semisynthetic derivatives, the compound that has reached further development has been the phosphate prodrug of *N*-acetylcolchinol **7** (ZD6126). This compound presented a higher vascular disrupting than antimitotic activity, but its clinical development has been halted due to severe cardiotoxicity.[28]

Combretastatin A-4, described by Pettit et al.[46] in 1995, is a *cis*-stilbene isolated from the bark of the African willow tree *Combretum caffrum*. Other combretastatins such as combretastatin A-1 (**8**, CA-1), with an extra OH on ring B,[21] or combretastatin A-2 (**9**, CA-2), with a methylenedioxy bridge at ring A[23] (Figure 4), described and studied by the same group, showed antivascular properties similar to CA-4. However, combretastatins are characterized by poor solubility and chemical instability. In the presence of light, heat, or acid media, but also after in vivo administration, the *cis*-stilbene easily isomerizes to the *trans*-stilbene (Figure 5) that is significantly less potent at inhibiting tubulin polymerization and cancer cell growth.[47] To improve solubility, prodrugs have been developed both for CA-4 and CA-1. The phosphate prodrugs CA-4P[22] (**10**, Zybrestat, Fosbretabulin) and CA-1P[48] (**11**, OXI4503) are currently being evaluated in phase II/III and

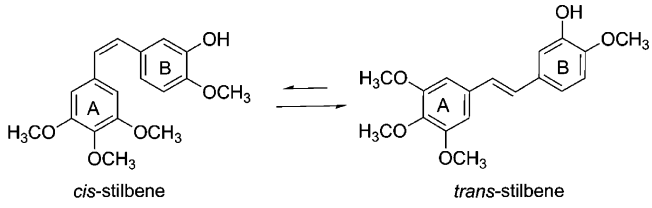

Figure 5. *Cis*–*trans* isomerization of CA-4.

phase I/II clinical trials, respectively, whereas ombrabulin (**12**), the serine derivative of 3′-amino-deoxycombretastatin A-4,[49] was discontinued in 2013 after disappointing results from phase III clinical trials (Figure 4). It is relevant to mention that CA-1, and by extension its prodrug, can undergo activation to a cytotoxic *ortho*-quinone intermediate that may interact with protein thiols and nucleic acids and stimulate oxidative stress through superoxide/hydrogen peroxide production.[50] This could help to explain the superior antitumor effect of CA-1 compared to CA-4 and illustrates how subtle differences in structure may account for the activation of different pathways relevant for the mechanism of action. We will refer to these prodrugs in a later section.

Most efforts addressing the synthesis of structural analogues of combretastatins have been directed to fix the conformation of the *cis*-stilbene connecting the two aromatic rings (Figure 6). It should be kept in mind that the 3,4,5-trimethoxy substitution pattern in ring A is required for optimal activity, while modifications at ring B are tolerated. Still, the 4-methoxy-3-hydroxy or 4-methoxy-3-amino patterns are the most abundant B-rings in those compounds with better activity.

A reasonable and highly explored approximation in order to stabilize the *cis*-disposition of rings A and B has been the incorporation of the stilbene into a *cis*-restricted bridge, as shown by the general formula **13** (Figure 6). A successful strategy has been the employment of (heterocyclic) rings, particularly through a five-membered ring, so that not only the conformation is fixed as *cis* but also the drug-like properties can be improved both in terms of solubility and chemical stability. Such heterocyclic rings include heteroaromatic rings like pyrazole, imidazole, thiadiazole, triazoles and tetrazoles, isozazoles, or 1,2,3-thiadiazoles, and a detailed revision of them can be found in Tron et al.,[35] Lu et al.,[36] and Rajak et al.[40]

DOI: 10.1021/acs.jmedchem.6b00463
J. Med. Chem. 2016, 59, 8685−8711

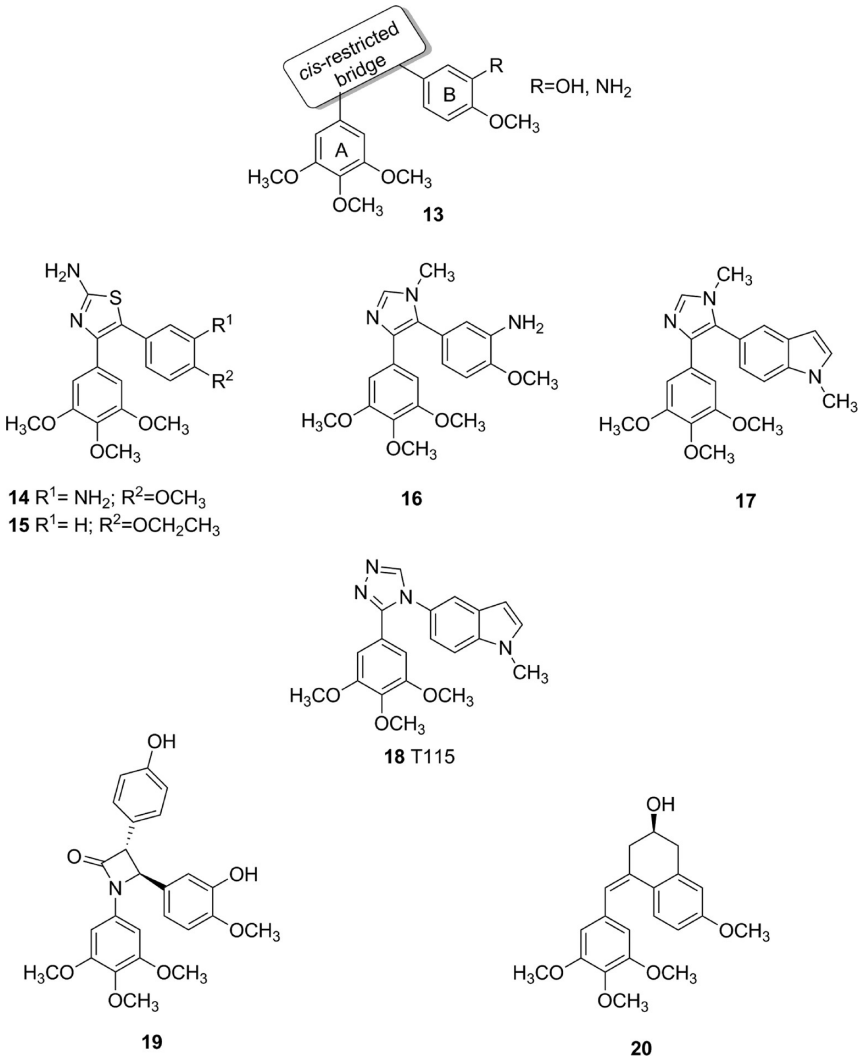

Figure 6. *Cis*-restricted bridged compounds mimicking CA-4.

Relevant examples include the 2-aminothiazoles, originally reported by Ohsumi[51] with compound **14** as a prototype and further explored by Romagnoli et al.,[52] affording compounds with IC_{50} values ranging from 0.03 to 0.9 nM (Figure 6). Particularly, compound **15** (TR644) was found to be superior to CA-4 in inhibiting tubulin polymerization (0.61 ± 0.07 versus 1.2 ± 0.1 μM for CA-4) while a perfect overlapping with colchicine was shown by competition experiments.[52]

Other interesting examples of *cis*-restricted bridges are the *N*-methyl imidazoles, as shown in compounds **16** and **17** (Figure 6). The rational in the design of these compounds was that the basic nitrogen on the imidazole ring might decrease lipophilicity while allowing the synthesis of water-soluble salts.[53] Indeed, compounds **16** and **17** showed cytotoxicity in the nM range and, more importantly, both compounds were found to present a good pharmacokinetic profile with high oral bioavailability and excellent in vivo activity against murine M5076 reticulum sarcoma tumors in mice.[53] It is also interesting to highlight the presence of an indole as ring B in compound **17**. In fact, this ring has been extensively employed as a B-ring alternative. It is also present in **18** (T115), reported by Welsh and co-workers,[54] where a 1,2,4-triazole has been used to restrict the conformation of the bridge linking rings A and B. Also in this case, inhibition of tubulin polymerization and disruption of a microtubule network, similar to CA-4, was reported. In a mouse xenograft model using HT-29 human colon carcinoma or PC3 prostate cancer cells, a significant inhibition of tumor growth was observed after intraperitoneal administration.[55]

Among nonaromatic heterocycles bridging rings A and B, the 2-azetidinones (β-lactams), described by Sun et al.,[56] have been proposed as a viable linking alternative. Indeed, compound **19**[57] (Figure 6) has shown antiproliferative activity in the sub-nM range and new compounds in this series still continue to be explored.[58] Compared to previous examples, these compounds include an additional substituent (an aryl in most cases as in **19**) and a *trans*-relationship between the substituents at positions 3 and 4.

Very recently, quantum mechanics calculations have been used to study the instability of combretastatin A-4,[59] leading to bicyclic derivatives at rings A or B as an alternative strategy to stabilize the *cis*-configuration. Compound **20** (Figure 6), belonging to this series, was found to provide IC_{50} values in the nM range in cell culture and to be active in HT-29 tumor-bearing nude mice.

Another highly explored way to link rings A and B has been through a simple carbonyl linker as exemplified by benzophenone derivatives. In such compounds, the carbonyl

DOI: 10.1021/acs.jmedchem.6b00463
J. Med. Chem. 2016, 59, 8685−8711

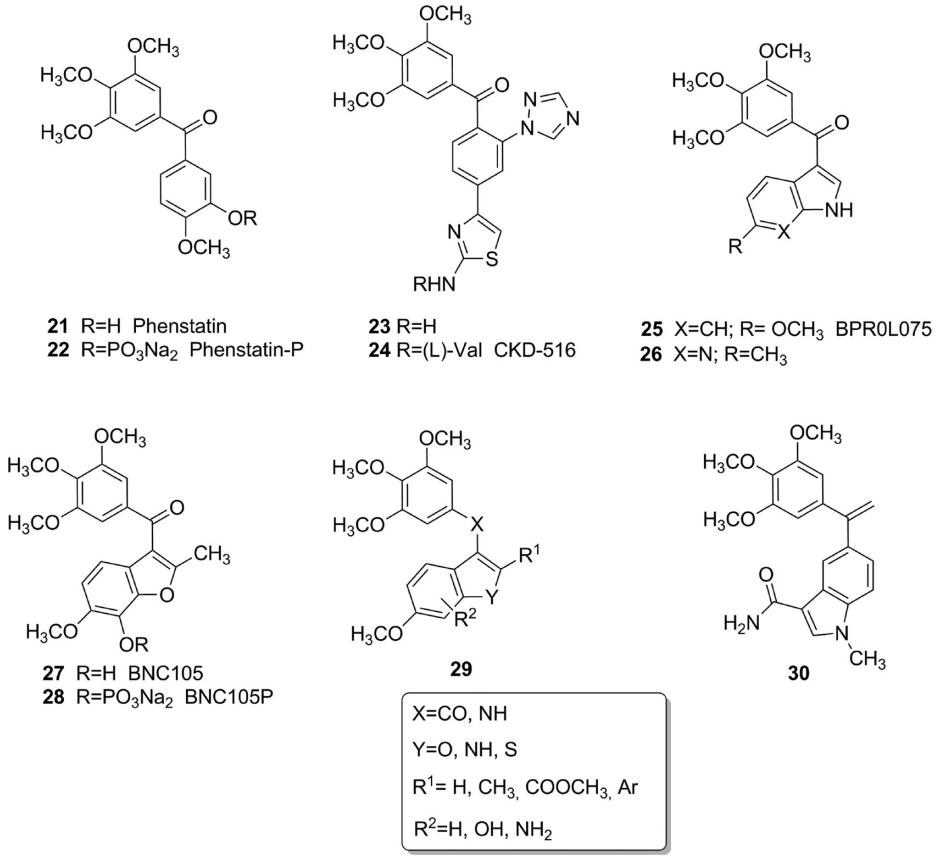

Figure 7. 1,1-Diaryl ketone derivatives mimicking CA-4.

function significantly constrains the relative conformation of the two aryl rings in a quasi *cis* orientation. Indeed, phenstatin (**21**, Figure 7) can be seen as the closest analogue to CA-4 among benzophenones. Phenstatin and its phosphate prodrug **22**[60] showed inhibitory values similar to those of CA-4P in antiproliferative assays, while binding to tubulin was equivalent to that of CA-4. Other relevant examples of benzophenone derivatives were provided by Lee and co-workers,[61] who explored the incorporation of different five-membered heterocycles at positions 2, 4, and 5 of ring B of the benzophenone with the aim to improve chemical stability and, particularly, solubility and PK values. Compound **23** (Figure 7) was identified as one of the most potent compounds in this series. Its L-valine prodrug **24** (CKD-516) further improved its aqueous solubility and showed marked antitumor efficacy against murine (CT26 and 3LL9) and human (HCT116 and HCT15) xenografts in mice. Encouraging results from phase I clinical trials following intravenous administration have just been published.[62]

Very close in structure to benzophenones are 1,1-diarylketones, some of which have provided very interesting VDA activities. As mentioned in previous series, in most cases ring A is kept almost intact with the 3,4,5-trimethoxy substitution pattern, where ring B has been replaced by bicyclic aromatic heterocycles. An early example in this series is **25** (BPROL075),[63] an indole derivative with IC_{50} values against a variety of human tumor cells in a single-digit nM range and activity in nude mice against xenografts of human gastric carcinoma MKN-45, human cervical carcinoma KB, and KB-derived P-gp170/MDR-overexpressing KB-VIN10 cells at intravenous doses of 50 mg/kg. Applying a scaffold-hoping approach looking for a backup drug candidate,[64] the 7-azaindole derivative **26** was synthesized, providing a significant improvement in oral bioavailability, metabolic stability, and aqueous solubility (as the HCl salt) although the antiproliferative activity was reduced 4-fold compared to **25**.

Another relevant example is the benzo[*b*]furane derivative **27** (BNC105),[65] structurally related to the indole and whose phosphate prodrug **28** (BNC105P) is being evaluated in phase II clinical trials. Compound **27** was selected by Kremmidiotis et al.[66] using an "in vitro" screening approach comparing the inhibitory activity of compounds on proliferating versus quiescent endothelial cells to improve the selectivity of VDAs. They reported that **27** displayed 80-fold higher potency against endothelial cells that were actively proliferating or forming capillary tubes compared with nonproliferating endothelial cells or endothelium found in stable capillaries, a selectivity that was not observed with CA-4.[66] It is interesting to highlight that, compared to CA-4, **27** exhibited a longer half-life, larger $AUC_{0-\infty}$, and a lower level of plasma protein binding, resulting in a higher free drug exposure.[65] The favorable pharmacokinetics and the wider selectivity compared to CA-4 are two important characteristics of **27**. It is also relevant to mention that the compound is cleared from healthy tissues over 24 h, but due to the vascular shutdown effect, a significant percentage of the drug is trapped in the tumor tissue after 24 h.[66]

The number of benzo[*b*]furanes, indoles, benzo[*b*]-thiophenes with or without substitutions at position 2 (represented by the general formula **29**, Figure 7), or alternative bicyclic heterocycles such as quinolines,[67] that have shown a CA-4 like behavior is very high. Detailed

DOI: 10.1021/acs.jmedchem.6b00463
J. Med. Chem. 2016, 59, 8685−8711

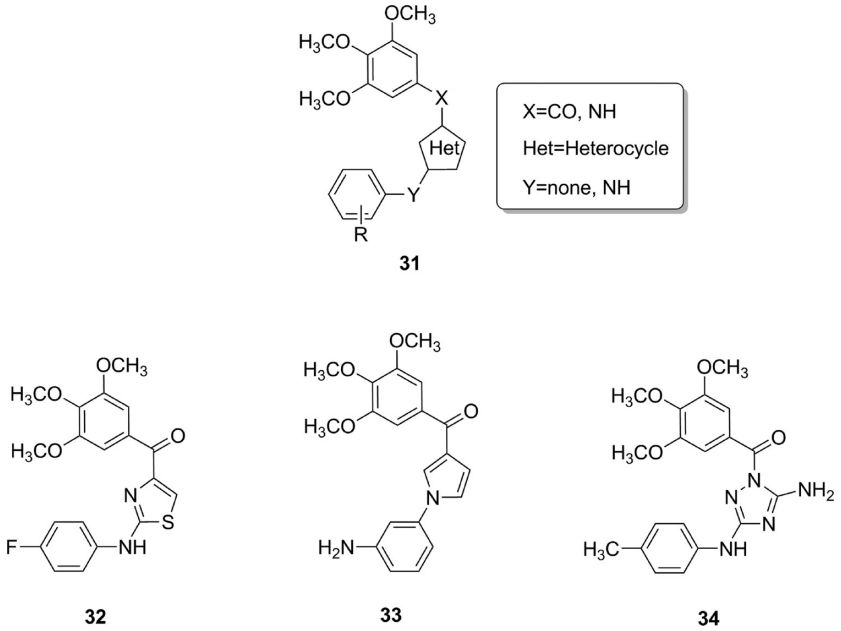

Figure 8. Other modifications at B-ring on 1,1-diarylketone derivatives.

structural and biological information about these compounds is covered in recent review articles.[36,40] Also, the linker connecting both aryl rings is susceptible to modifications including sulfide, amine, sulfonamide, or ether linkages (as represented by the general formula **29**). Very recently, selenium has also been used as a linker.[68] In many cases, the ketone provides the best inhibitory activity, but there are examples where an NH[69] or a sulfur linkage[70] also provides potent colchicine site binders with antiproliferative activity in the nM range. Very close in structure to 1,1-diarylketones are 1,1-diarylethenes, also designated as isocombretastatins. As a representative example, we refer to compound **30**, described by Alvarez et al.,[71] which shows antiproliferative activity in the sub-nM range and where the incorporation of the amide functionality at position 3 of the indole is meant to improve solubility.

In these 1,1-diaryl ketone derivatives, ring B can be replaced by a five-membered heterocycle that is additionally substituted by an aryl ring directly attached to the heterocycle or linked through an NH and represented by the general formula **31** (Figure 8). Examples of this series have been reported by different groups: the so-called PAT-compounds (as **32**)[72] where pharmacokinetic parameters are improved compared to previous series, the ARAP derivatives (as **33**)[73] that have also the potential to strongly inhibit the Hedgehog signaling pathway, or the 3-arylamino-5-amino-1,2,4-triazoles (as **34**) that have hampered the growth of syngeneic hepatocellular carcinoma in Balb/c mice.[74]

Chalcones represent another important group of colchicine site binders. They are abundantly present in natural products as precursors of flavonoids. Their biological activities are very diverse and include antitumoral properties.[75] The antimitotic activity of chalcones and their capacity to affect tubulin assembly have been reviewed.[76] Chalcones mimicking the substitution pattern of CA-4, such as **35** (Figure 9), have been reported by Ducki et al.,[77] showing antiproliferative activity in the nM range. More recently, chalcone **36** has shown in vivo antitumor activity in A549 tumor xenograft models. Interestingly, compound **36** and similar analogues were found to

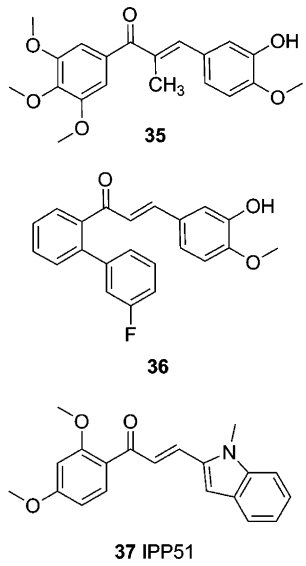

Figure 9. Chalcone derivatives with a combrestastatin-like behavior.

exhibit affinity-induced fluorescence during tubulin-binding.[78] Also within chalcones, the B-ring can accommodate indol rings, as exemplified by **37** (IPP51)[79] that inhibited tumor growth in a human bladder xenograft model. Other examples where the bridge connecting rings A and B contains a pyridine have been described by Zheng et al.[80]

2.4.2. Noncombretastatin Colchicine-Site Binders. Up to here, the compounds described might be considered as "inspired" by the structure of combretastatins. In this section, we will refer to compounds that are structurally unrelated to CA-4 but that have proven to efficiently bind tubulin at the colchicine site and behave as VDAs. We have centered our attention at those compounds that have reached clinical trials.

The sulfonamide **38** (ABT-751, E7010) (Figure 10) was reported as a colchicine site binder already in 1997,[81] around the same time the antivascular activity of CA-4 was described. This compound is active against a broad range of tumor cell

DOI: 10.1021/acs.jmedchem.6b00463
J. Med. Chem. 2016, 59, 8685−8711

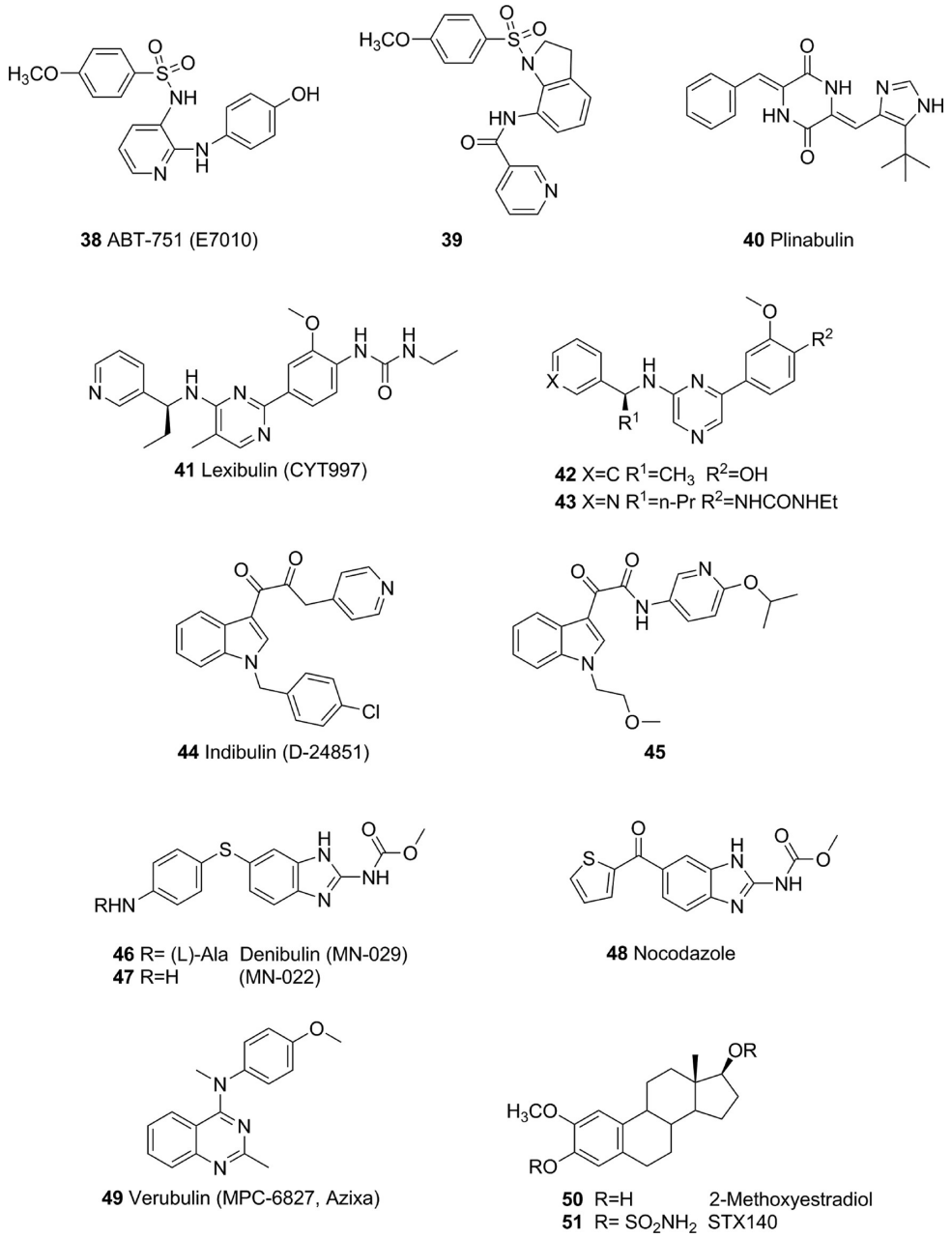

Figure 10. Colchicine-site binders structurally different from CA-4.

lines in vitro and in xenograft models of human gastric, colorectal, lung, and breast cancer in vivo.[82] In addition, compound **38** is well absorbed after oral administration with an overall mean T_{max} of about 2 h, and results from phase I clinical trials were reported in 2006.[82] However, more recent results on phase I/II trials were quite discouraging.[28] The sulfonamide **38** is also one of the first examples, besides DAMA−colchicine, whose complex with $\alpha\beta$-tubulin has been solved by X-ray crystallography.[83] Other sulfonamides are being explored, like **39**.[84] This compound can be seen as a conformationally constrained analogue of **38** and is also a potent tubulin inhibitor and orally bioavailable.

Plinabulin (**40**, NPI-2358) is a hydrophilic synthetic diketopiperazine arising from phenylahistin, a natural product isolated from *Aspergillus* sp.[85] Plinabulin exhibits potent antiproliferative activity against a panel of tumor cell lines in the low nM range and induces tubulin depolymerization. Because docking studies did not provide clear insights into the binding mode to tubulin, some chemical probes incorporating biotin and benzophenone were synthesized and used for photoaffinity studies.[86,87] Such studies finally concluded that plinabulin interacts in the boundary region between α- and β-tubulin near or at the colchicine binding site.[87] An X-ray crystal structure of the recently solved complex[88] has afforded additional information on this subject. It is interesting to highlight that one of the requirements for activity among plinabulin derivatives is the presence of a rigid and planar pseudotricyclic structure formed by a hydrogen bond between the NH of the diketopiperazine and the N of the imidazole.[89] Such pseudotricyclic structures have also been proposed as a requisite for tubulin binding by unrelated compounds such as 1-aroylnaphthalene derivatives[90] or cyclohexanediones.[32,33] Results from phase I/II clinical trials with plinabulin are detailed in other reviews.[26,28]

DOI: 10.1021/acs.jmedchem.6b00463
J. Med. Chem. 2016, 59, 8685−8711

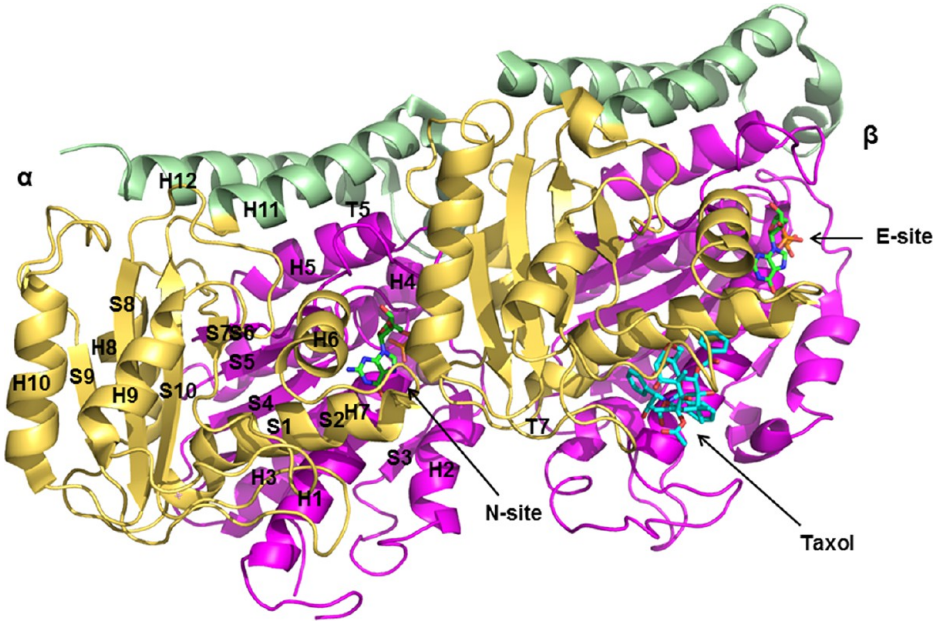

Figure 11. Structure of $\alpha\beta$-tubulin in complex with taxol (PDB code 1JFF). Color code for the domain in each monomer: N-terminal in magenta, intermediate domain in orange, and C-terminal domain in green. Taxol (cyan), GDP, and GTP (green) are shown in sticks.

Lexibulin (**41**, CYT997) is another colchicine site binder tested in phase I/II clinical trials and whose development has been discontinued. Its complex with tubulin has just been solved.[88] The discovery of lexibulin started with the identification of the pyrazine analogue **42** while screening the antiproliferative activity of Cytopia's library.[91] By performing a focused analogue medicinal chemistry program, a 1000-fold more potent analogue with activity in the nM range (**43**) was identified. However, its solubility and pharmacokinetics were unacceptable. By replacing the core heteroaromatic ring pyrazine to a pyrimidine and by incorporation of a methyl substituent, as shown in **41**, potent antiproliferative activity was maintained while accompanied by a good pharmacokinetic profile.[91] Additional biological studies confirmed its VDA activity, with in vivo effects on tumor blood flow.[92]

Indibulin (**44**, D-24851) is another example of a compound class differing from colchicine and CA analogues, identified in a cell-based screening assay to discover cytotoxic drugs. Indibulin has potent cytotoxicity activity in vitro against different human tumor cell lines and in vivo after oral administration to rats bearing Yoshida AH13 sarcomas.[93] Results from phase I clinical trials indicated a plateau in drug exposure prior to reaching the maximum tolerated dose, probably related to its poor aqueous solubility.[94] In this sense, there is a very recent article on indole-3-glyoxylamides that addresses solubility improvement among this series by reducing the number of aromatic rings and increasing the count of sp^3 atoms, exemplified by compound **45**.[95] Significant growth inhibition in a mouse model of head and neck cancer has been reported for **45**.[95]

Denibulin (**46**, MN-029) is the L-alanine prodrug of **47** (MN-022). Rapid metabolization of **46** to the free amine **47** and its *N*-acetyl derivative has been described. Phase I clinical trials further showed that denibulin is well tolerated and is able to decrease tumor vascular parameters following intravenous infusion.[96] It is interesting to highlight that the structure of **47** very much resembles that of nocodazole (**48**), a well-known tubulin-depolymerizing agent whose complex with $\alpha\beta$-tubulin has recently been solved.[88]

Verubulin (**49**, MPC-6827, Azixa) represents another interesting VDA that has reached clinical trials and whose structure significantly differs from that of CA-4 and analogues. This quinazoline derivative was identified through a HTS campaign meant to identify proapoptotic compounds.[97] Its antimitotic properties were shown to be a consequence of the binding to $\alpha\beta$-tubulin at the colchicine site. Verubulin showed a high blood–brain barrier penetration[98] and has been detected in the cerebrospinal fluid. However, its high lipophilicity required a formulation with significant side effects, so clinical trials have been suspended. It has recently been highlighted[99] that a similar substitution pattern to that of verubulin is observed in fused-pyrimidine derivatives reported by Gangjee et al.[100,101] that not only target tubulin but are able to inhibit receptor tyrosine kinases involved in angiogenesis such as vascular endothelial growth factor receptor-2 (VEGFR-2) and platelet-derived growth factor receptor β (PDGFR-β).

2-Methoxyestradiol (**50**, 2-ME) is an endogenous estrogen metabolite implicated in different processes including inhibition of tumor vascularization and growth by binding at the colchicine site.[102] However, its rapid metabolization and poor pharmacokinetics have launched the synthesis and biological evaluation of novel analogues. As an interesting example, we include the bis-sulfamate **51** (STX140)[103] with excellent oral bioavailability and whose mechanism of action, besides binding tubulin, seems to involve other targets including carbonic anhydrase.[104] Other compounds being explored in this series include steroidomimetic tetrahydroquinolines[105] or steroid derivatives substituted at positions 3 and 17, positions that are quickly metabolized in methoxyestradiol.[106]

3. X-RAY STRUCTURES OF TUBULIN AND TUBULIN–COLCHICINE SITE LIGANDS

3.1. Tubulin Structure. Tubulin is a heterodimer constituted of two monomers of 50 Kd designated as α and β subunits, with ca. 40% sequence identity between them. The first structural studies on the $\alpha\beta$-tubulin dimer appeared in 1998, when Nogales et al.[107] reported a three-dimensional

DOI: 10.1021/acs.jmedchem.6b00463
J. Med. Chem. 2016, 59, 8685–8711

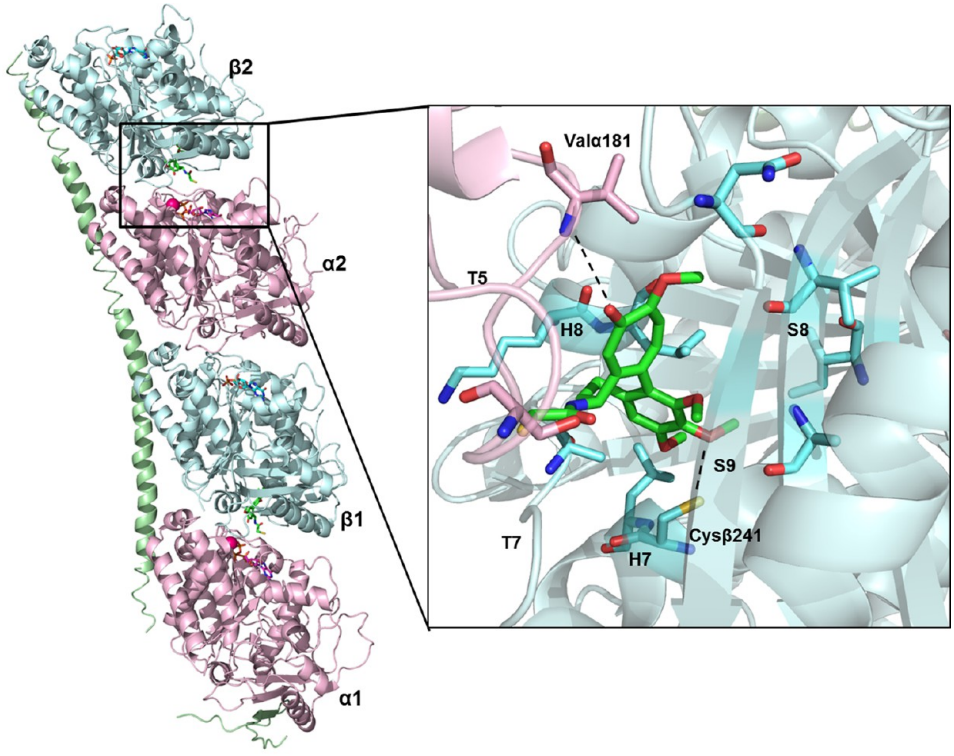

Figure 12. Overall structure of the DAMA−colchicine−tubulin complex and detailed insight into the binding mode of DAMA−colchicine. The α subunit is represented in light pink and the β subunit in light cyan. Colchicine is represented in green in sticks, and relevant amino acids at the colchicine site are also represented in sticks.

model fitted to a 3.7 Å density map obtained by electron crystallography of zinc-induced tubulin sheets stabilized with taxol. The atomic model of the tubulin dimer, in a straight conformation, was further refined to 3.5 Å resolution.[108] In this model, the α and β subunits of tubulin presented the same overall compact structure, where each monomer could be divided into three domains (Figure 11). The N-terminal domain (residues 1−205, magenta in Figure 11) contains the nucleotide-binding domain and comprises six parallel β-strands (S1−S6) alternating with six helices (H1−H6). The loops (T1−T6) joining strands and helices are directly involved in the binding of the nucleotide. The interaction of the N-terminal end of the core helix H7 with the second, smaller domain (residues 206−381, yellow in Figure 11), designated as intermediate domain, formed by three helices (H8−H11) and a mixed β-sheet (S7−S10), completes the nucleotide-binding site. The C-terminal domain (residues 385 to the c-terminus, green in Figure 11) contains two antiparallel helices (H11−H12) that cross over the two other domains. This domain finishes with the highly acidic tail. Sequence variability in this C-terminal tail is related to the different isotypes of tubulin (six forms of α-tubulin and 7 forms of β-tubulin).[109]

Each tubulin monomer binds a guanine nucleotide. The nonexchangeable GTP is bound into the α subunit in the so-called N-site buried at the dimer interface, while the exchangeable GDP is bound into the β subunit (namely E-site) exposed on the surface of the dimer.

In 2000, using X-ray crystallography, Gigant et al.[110] were able to determine the structure of two $\alpha\beta$-tubulin dimers in complex with the stathmin-like domain of the neural protein RB3 (RB3-SLD) at 4 Å. In the overall structure, the RB3 protein adopted a hook-like shape able to accommodate two tubulin heterodimers so that the complex formed a curved structure that, as will later be discussed, has important consequences. Each dimer contained GTP and GDP molecules located inside α and β subunits, respectively. The strategy to use stathmin or other "tubulin sequestration" proteins to stabilize the complex has been critical in solving the structure of tubulin with different ligands.

3.2. Overview of Colchicine−Tubulin Complexes Based on X-ray Data. Although the structure of the tubulin−taxol complex was already reported in the late 1990s,[107] atomic details of the colchicine-binding site became apparent only in 2004 when Ravelli et al.[18] solved the structure of $\alpha\beta$-tubulin with the stahmin-like domain of the RB3 protein in complex with *N*-deacetyl-*N*-(2-mercaptoacetyl)colchicine (DAMA−colchicine, PDB code 1SA0) (Figure 12), indicating that the *N*-acetyl group of DAMA−colchicine (**52**, Figure 13) was definitive to unambiguously define the colchicine orientation in its asymmetric density. This pioneering work unraveled that the DAMA−colchicine binding site was located close to the interface between the α and β subunits of each tubulin dimer, mostly buried in the intermediate domain of the β subunit and boxed in by strands S8, S9, helices H7 and H8, and loop T7 from this subunit (Figure 12). In this binding mode, the methoxy group of ring A of DAMA−colchicine establishes a hydrogen-bond interaction with Cysβ241, while ring C interacts with loop T5 of the N-terminal nucleotide-binding domain of the α subunit by a H-bond between the carbonyl group of ring C and the backbone of Valα181. This model could also explain how colchicine binding might affect tubulin dynamics. The ternary tubulin−podophyllotoxin:RB3-SLD complex (**6**, Figure 13, PDB code 1SA1) was also described.

DOI: 10.1021/acs.jmedchem.6b00463
J. Med. Chem. 2016, 59, 8685−8711

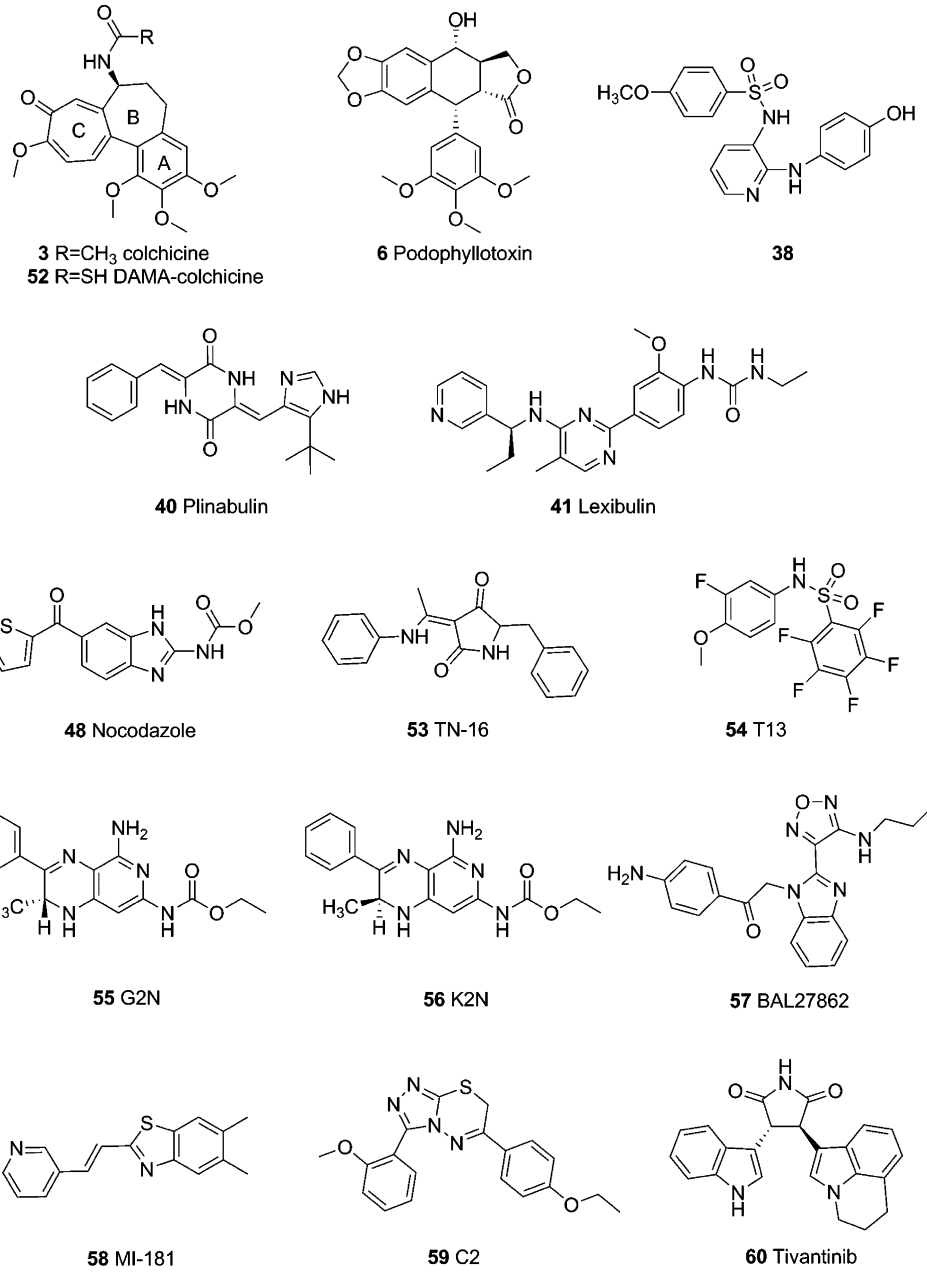

Figure 13. Chemical structures of colchicine site ligands cocrystallized with $\alpha\beta$-tubulin.

In 2009, making use of the RB3-SLD complex, the same research group reported on a set of structures that included an unliganded tubulin (PDB code 3HKB) and complexes with three known colchicine site ligands: the sulfonamide **38** (PDB code 3HKC), the pyrrolidinedione **53** (TN-16, PDB code 3HKD), and the pentafluorophenyl derivative **54** (T13, PDB code 3HKE)[83] (chemical structures in Figure 13). In all cases, van der Waals contacts between the ligand and the protein proved to be the most relevant for the interaction, while polar interactions were very few. The binding of **38** very much resembles the binding of colchicine, although **38** is more hidden in β-tubulin than colchicine with no contacts with the α-subunit. Concerning the binding of **53** (Figure 14), the ligand appears much more deeply buried in the β subunit, limiting the overlap to DAMA−colchicine only to the subsite where the colchicine A-ring is located. Therefore, **53** establishes fewer contacts with the tubulin intermediate domain, while making new interactions with the β strands S4, S5, and S6 of the nucleotide-binding domain of β tubulin. Because of the accessory pocket explored by **53** inside the β subunit of tubulin, these new structures allowed expansion of the definition of the colchicine-binding site to the more extensive term designated "colchicine-binding domain".[83] Moreover, it was possible to identify local changes that contributed to tubulin curvature in the absence of colchicine site ligands. Local conformational changes were observed when the structures of the unliganded curved tubulin (T2RB3) and the colchicine−tubulin complex (T2RB3−colchicine) were compared.[18] While the overall structure and curvature remained unchanged, a switch of the T7 loop was observed (Figure 15). This loop lies in the colchicine site when it is empty but moves toward the dimer interface upon ligand binding.

In 2010 Barbier et al.[111] demonstrated that the buried cavity described for **53** was also occupied by **55** (G2N, Figure 13,

DOI: 10.1021/acs.jmedchem.6b00463
J. Med. Chem. 2016, 59, 8685−8711

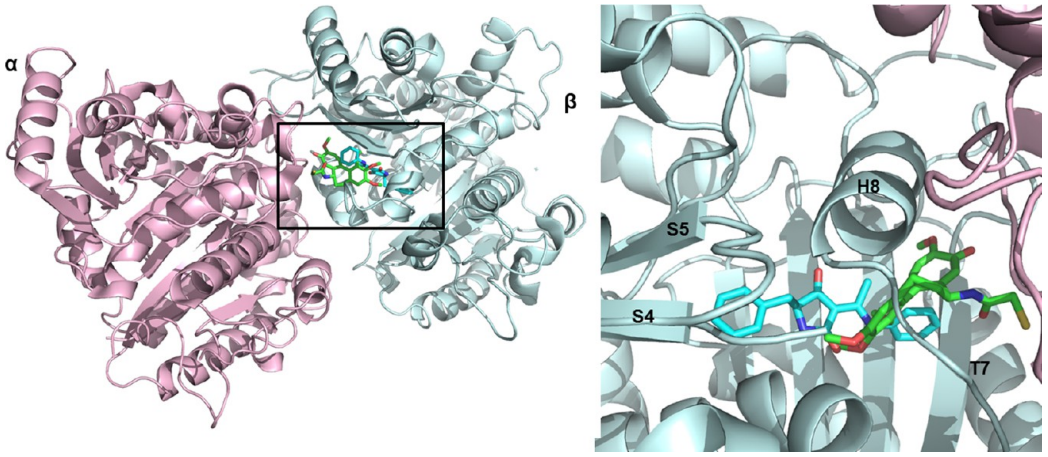

Figure 14. (a) Crystal structure of the complex of tubulin with the pyrrolidinedione **53**. The α subunit of tubulin is represented in light pink and the β subunit in light cyan. (b) View of the binding mode of **53** represented in sticks (cyan) after a 180° rotation. For comparison, DAMA−colchicine is shown in green sticks.

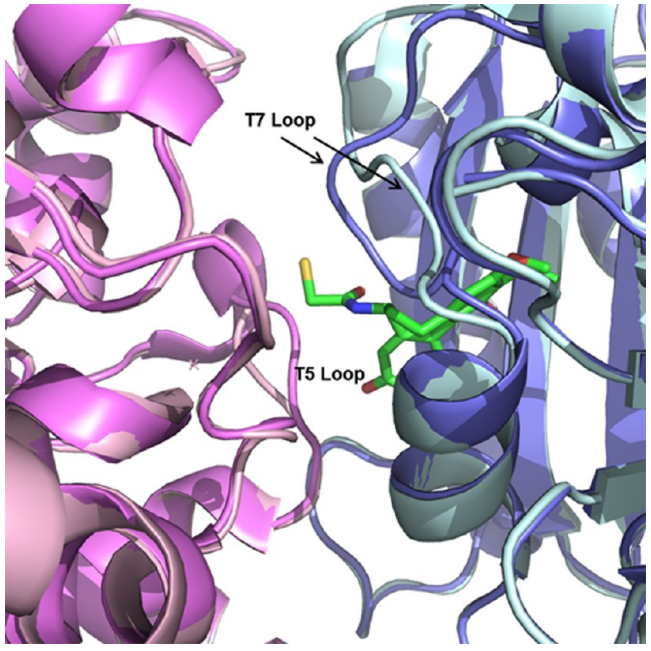

Figure 15. Conformation change of the T7-loop upon colchicine binding. α-Tubulin in the unbounded state is represented in magenta and β-tubulin is represented in blue; the α-tubulin in the colchicine complex is represented in light pink, while β-tubulin is represented in pale cyan.

PDB code 3N2G) and **56** (K2N, Figure 13, PDB code 3N2K), the chiral *R* and *S* isomers, respectively, of the mitotic inhibitor ethyl-5-amino-2-methyl-1,2-dihydro-3-phenylpirido[3,4-*b*]-pyrazine-7-yl-carbamate.

It should be mentioned that all the complexes discussed so far have a low-to-medium resolution, with values between 3.58 and 4.20 Å. More recently, higher-resolution structures (<2.5 Å) have been obtained by Steinmetz's group using tubulin tyrosine ligase (TTL), a well-known enzyme involved in the post-translational modifications at the C-terminal tail in tubulin,[109,112] as an additional structural protein. Therefore, crystals containing two heterodimers of tubulin (T2), the stathmin-like domain of RB3 (R), and TTL were solved at 2.6−1.8 Å resolution.[113] Moreover, by using soaking techniques, T2RTTL complexes of either microtubule stabilizing[114] or destabilizing ligands[115,116] have been reported. In particular, the complexes of T2RTTL with **57** (BAL27862, Figure 13, PDB code 4O2A) and with colchicine (**3**, PDB code 4O2B) were solved at 2.5 and 2.3 Å resolution, respectively.[115]

During the last year, using the protein complex T2RTTL, other authors have determined the structures of structurally diverse colchicine site binders. Particularly the complexes with **58** (MI-181, Figure 13, PDB code 4YJ2) and **59** (C2, PDB code 4YJ3)[117] were reported in 2015, while early this year additional complexes with lexibulin (PDB code 5CA0), nocodazole (PDB code 5CA1), plinabulin (PDB code 5C8Y), and tivantinib (**60**, PDB code 5CB4) have been published.[88] Surprisingly, although CA-4 is considered the prototype and best studied VDA, to date, no X-ray structural data of its binding mode with tubulin are available.

3.3. Structural Details of the "Colchicine Domain".

The colchicine-binding site is a deep pocket, mostly buried in the intermediate domain of the β subunit, located near the interface between α and β subunits of a tubulin dimer. As already mentioned, the comparison between the crystal complexes of DAMA−colchicine and **53** with tubulin led to the proposal that colchicine site ligands bind to tubulin in a "colchicine domain" which comprises a main site (where colchicine itself binds) and additional neighboring pockets.

Massaroti et al.[43] nicely analyzed by structural interaction fingerprints (SIFt)[118] this colchicine-binding domain and proposed a division into three zones, designated as zones 1, 2, and 3, as shown in Figure 16a. Zone 1, considered an accessory pocket, is facing the α subunit interface, surrounded by residues Valα181, Serα178, Metβ259, and Asnβ258. Zone 2, or the main zone (in the center of the domain, Figure 16a), is a hydrophobic pocket located in the β subunit formed by residues Lysβ352, Asnβ350, Ileβ378, Valβ318, Alaβ317, Alaβ316, Leuβ255, Lysβ254, Leuβ252, Alaβ250, Leuβ248, Leuβ242, and Cysβ241. Finally, zone 3, the second accessory pocket, is buried deeper in the β subunit and is formed by residues Thrβ239, Valβ238, Tyrβ202, Gluβ200, Pheβ169, Asnβ167, Glnβ136, and Ileβ4.

Taking the crystal structure of colchicine complexes as reference, colchicine-domain ligands (CDLs) can be divided into two main groups. There are a number of ligands (**6**, **38**, **41**, **54**, **57**, and **60**, Figure 13) that bind similarly to colchicine, occupying zones 1 and 2. A superposition of their binding

DOI: 10.1021/acs.jmedchem.6b00463
J. Med. Chem. 2016, 59, 8685−8711

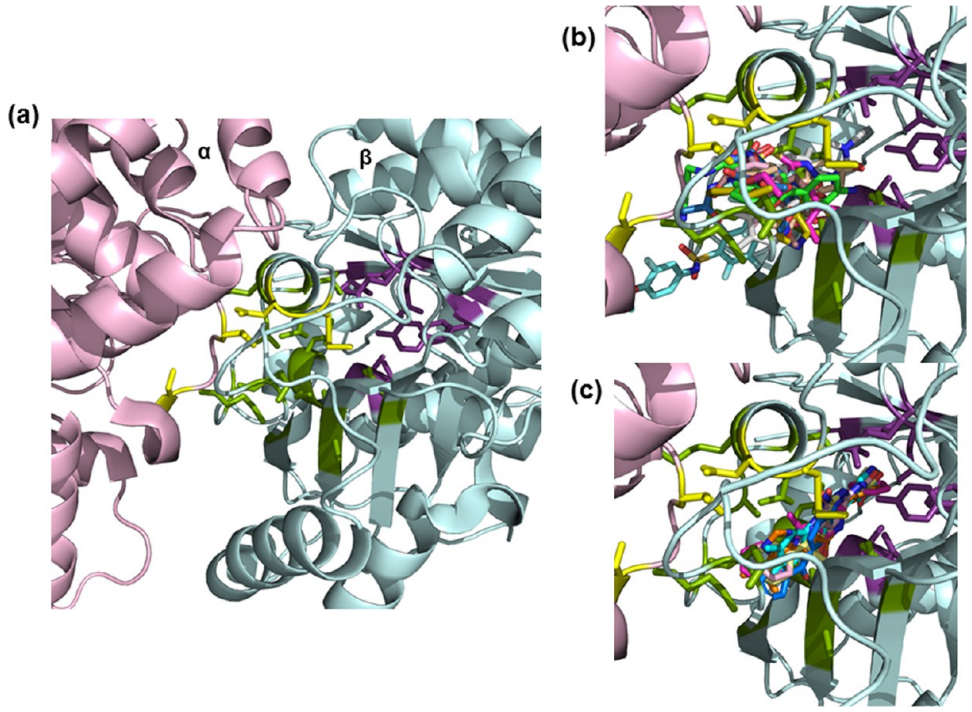

Figure 16. (a) The colchicine-binding domain. The α subunit of tubulin is represented in light pink and the β subunit in light cyan. Residues from zone 1 (yellow), zone 2 (green), and zone 3 (violet) are shown in sticks. (b) Superposition of the ligands mimicking the colchicine-binding mode: **6** (brown), **38** (light orange), **41** (white), **52** (blue), **54** (light-pink and cyan), **57** (green), **59** (pink), and **60** (yellow). (c) Superposition of ligands mimicking the pyrrolidinedione-binding mode: **40** (orange), **48** (marine blue), **53** (pink), **55** (light pink), **56** (light yellow), and **58** (cyan). For chemical structures of the ligands, see Figure 13.

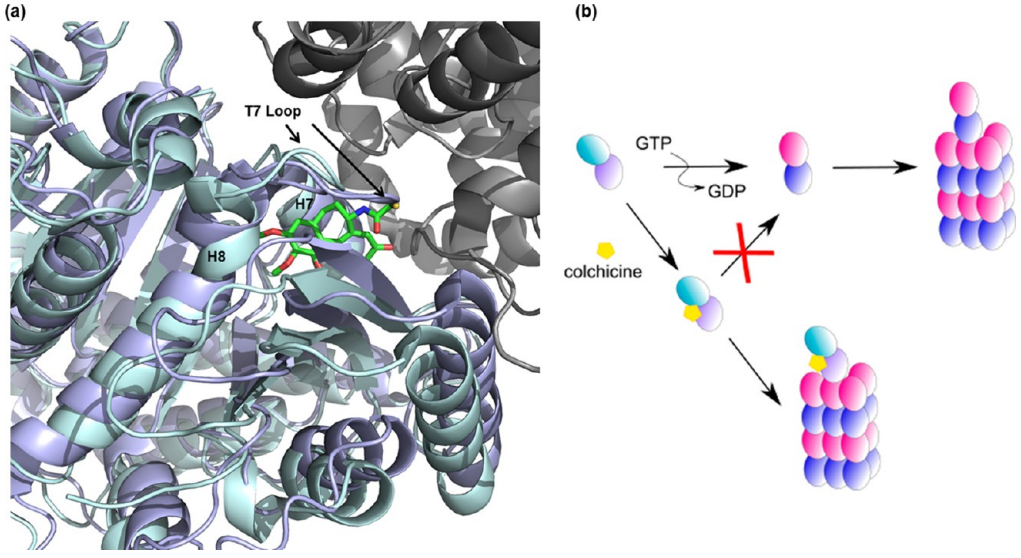

Figure 17. (a) Superposition of the N-terminal domain of β-subunits of the straight (slate blue) and curved (light cyan) conformations of tubulin. The α-subunit of the straight state is shown in gray, and colchicine is shown in sticks (green). In the straight tubulin (slate blue), the T7-loop occludes the colchicine site when compared to the curved tubulin (light cyan). (b) Curved-to-straight conformational transition of $\alpha\beta$-tubulin upon GTP binding required for microtubule growth. Binding of colchicine (represented by a yellow pentagon) into the $\alpha\beta$-tubulin dimer prevents the conformational transition and suppresses microtubule dynamics.

modes can be seen in Figure 16b. The second group collects a number of ligands (**40**, **48**, **55**, **56**, and **58**, Figure 13) that mimic the binding of the pyrrolidinedione **53**, occupying zones 2 and 3, and whose superpositions are shown in Figure 16c. When comparing the superposition in Figure 16b,c, it could be argued that planar compounds tend to locate deeper into the β-subunit making use of zones 2 and 3, whereas more globular or butterfly like shaped ligands occupy zones 1 and 2, mimicking the colchicine-binding mode. Moreover, none of the available crystal complexes shows ligands that occupy the entire colchicine domain.

It should also be mentioned that the pentafluorophenyl derivative **54** has been reported to covalently bind to tubulin.[83] Moreover, two binding modes have been described in the same

DOI: 10.1021/acs.jmedchem.6b00463
J. Med. Chem. 2016, 59, 8685−8711

crystal, shown in white in Figure 16b and in cyan in Figure 16c. Finally, the reader is referred to the original publications for a more detailed description of the binding mode of each of these ligands.

3.4. Microtubule Destabilization by CDLs: Straight versus Curved Tubulin. As mentioned before, tubulin dimers in microtubules adopt a straight conformation[107,108] while a curved conformation is found for tubulin in solution.[119,120] Therefore, a "curved-to-straight" structural transition of the $\alpha\beta$-tubulin dimer is required for microtubule formation and needs the rearrangement of several secondary structural elements, especially concerning the intermediate domain.[18,83] Moreover, the comparison of the curved tubulin−colchicine structure with the straight state of tubulin[18] (Figure 17a) shows that this conformational change in tubulin leads to the movement of the T7-loop toward the colchicine site, closing the cavity. This switch in the T7-loop suggests that colchicine cannot bind into tubulin in preformed microtubules,[18,83] although tubulin−CDL complexes can be incorporated into growing microtubules.[121] Thus, the microtubule-destabilizing activity of CDLs should consist in preventing the curved-to-straight transition in tubulin by the bound ligand, thus perturbing the microtubule end (Figure 17b). This behavior differs from other microtubule-destabilizing agents that do not behave as VDAs, such as vinca alkaloids, that bind at the interdimer interface and destabilize microtubule ends by producing a molecular wedge between two longitudinally aligned tubulin dimers, inducing curved protofilament assemblies incompatible with the straight conformation in microtubules.[122] It is conceivable that these differences in destabilizing tubulin might account for the distinctive biological activities of vinca alkaloids and colchicine-based VDAs.

4. PRODRUGS AND OTHER APPROACHES TO IMPROVE DRUG DELIVERY

As shown in previous sections, combretastatins and most of their structural derivatives suffer from very low solubility so that prodrug formulation has been a must in order to progress to preclinical evaluation. For compounds containing a phenolic OH, such as CA-4 (**4**), CA-1 (**8**), phenstatin (**21**), or the benzofurane derivative **27**, the most applied strategy has been the derivatization as phosphate prodrugs, as recently summarized by Boyle et al.[123] Such prodrugs have good chemical stability and are rapidly converted to the active drug in vivo due to the action of phosphatases. As an illustrative example, the half-life of CA-4P (**10**) is just a few minutes and the prodrug needs to be administered by infusion. Metabolism of CA-4 includes *Z* to *E* isomerization, *O*-demethylation, and glucuronidation, as recently reviewed.[25] Certainly, CA-1P (**11**) represents a particular case. As mentioned, CA-1 and its diphosphate prodrug have remarkable cytotoxicity, superior to that of CA-4. It has been proposed that this increased activity can be partially ascribed to its rapid metabolization, giving rise to reactive quinones. Still, it is difficult to quantify the contribution of these now well-characterized quinones to the overall antitumor activity of CA-1.[124]

Although the derivatization as phosphates has clearly improved the aqueous solubility of CA-4 and CA-1, the resulting prodrugs are charged at physiological pH and are cleaved by nonspecific phosphatases. Thus, phosphate prodrugs work nicely when administered parentally, but oral administration is generally unsuccessful.[125]

If the derivatization point in the parent drug is an amino group, coupling to amino acids is the reaction of choice, so that the prodrugs are cleaved by the action of aminopeptidases. The most relevant example in this series is ombrabulin (**12**), the serine derivative of 3′-amino-deoxycombretastatin A-4, a prodrug that has reached clinical trials. Pharmacokinetics have confirmed the rapid conversion of ombrabulin to its active amino metabolite so that the mean half-life of the prodrug is 12 min.[126] Interestingly, the terminal half-life of the active metabolite was 8 h. This supports a greater metabolic stability of the amine-derived combretastatin analogues and derivatives in comparison with their OH counterparts. Intravenous infusion was also the way of administration for ombrabulin in the reported clinical studies.

Another example is **24**, an L-valine prodrug of a 2-aminothiazole derivative. Derivatization as prodrug made it feasible to get the solubility required for in vivo studies.[61] Results from phase I clinical trials[62] indicate that after intravenous infusion, biotransformation to the amino derivative was almost complete, with only <1% of unchanged **24** being excreted in the urine, whereas the half-life of the active amino metabolite ranged from 4 to 6 h.

An interesting approach in the design of prodrugs is the work performed by You and co-workers[127] using photo-unclick chemistry to develop light-activatable prodrugs of combretastatin A-4. These prodrugs combine in their structure folic acid as a tumor targeting unit for folate receptor uptake, phthalocyanine as a photosensitizer and reporter, and the aminoacrylate bond as the linker for singlet-oxygen drug release. In addition, the length of the polyethylene spacer helps in the uptake of the prodrug by the tumor cells. The results obtained indicate that after prodrug administration to mice inoculated with folate-receptor colon 26 tumors and only after laser irradiation, a significant and selective antitumor effect was observed.[127]

Another way to improve the poor aqueous solubility and pharmacokinetic properties of CA-4 has been through alternative delivery systems such as polymeric micelles,[128] liposomes,[129] dendrimers,[130] or pH-sensitive nanocarriers.[131] These systems do not only improve the solubility and pharmacokinetics but may allow the delivery of CA-4 to a particular cell population, using targeted drug delivery systems. One of the most cited and bright examples with this aim is the work reported by Sengupta et al. on a nanoscale delivery system, designated "nanocell" that enables the temporal release of CA-4 and doxorubicin.[132] A more recent example directed toward a particular cell population involves nanocomplexes in which CA-4 or 2-ME have been encapsulated in poly(D,L-lactic-*co*-glycolic acid)-*b*-poly(ethylene glycol) (PLGA-*b*-PEG). The targeting moiety cetuximab, an antiepidermal growth factor receptor (EGFR) chimeric monoclonal antibody, is incorporated on the surface of the resulting coronas, which enables the targeted delivery to human hepatocellular carcinoma cells overexpressing the EGFR.[133]

Another interesting approach also in the nanomedicine field has been the coadministration of CA-4P with functionalized nanoparticles by exploiting the enhanced permeability and retention (EPR) effect. According to Song et al.,[134] in this system, CA-4P eradicates tumor cells in the central region of the solid tumor while the *cis*-diaminedichloroplatinum (CDDP) loaded nanoparticles (CDDP-NPs) mainly act at the tumor periphery. In vivo experiments using mouse xenograft models bearing C26 and MDA-MB-435 tumors evidenced that the coadministration shows a significantly higher anticancer efficacy compared to CDDP-NPs or CA-4P alone.[134]

DOI: 10.1021/acs.jmedchem.6b00463
J. Med. Chem. 2016, 59, 8685−8711

Related to this, it may be relevant to introduce the so-called "pharmacokinetic approaches" to cancer treatment, a concept that has also been recently reviewed.[135] According to this approach, it should be considered that intratumoral pharmacokinetics within solid tumor microregions are crucial for efficacy of the treatment regimens: not only the biophysical properties of the intratumoral microenvironment significantly differ from normal tissues, but treatment with antivascular agents as CA-4 or **27** may further alter this microenvironment. This should be taken into account when selecting the combination protocol, drug doses, treatment sequence, and/or durations.[135]

5. BIOLOGICAL ACTIVITIES THAT CONTRIBUTE TO THE ANTITUMOR ACTIVITY OF COMBRETASTATIN A-4

As mentioned earlier in this Perspective, key to the antitumor activity of CA-4 is the inhibition of tubulin polymerization thereby impairing the formation of functional microtubules, which are crucial to cell division, morphology, and movement. In particular, the tubulin-depolymerizing activity of CA-4 leads to (i) inhibition of endothelial and tumor cell mitosis, followed by mitotic catastrophe and/or apoptosis, (ii) cytoskeleton disruption of endothelial cells, resulting in endothelial cell shape changes, increased blood vessel permeability, and/or thrombus formation and vascular collapse, and (iii) inhibition of cell migration, resulting in antimetastatic activity. In the following sections, the different processes and molecular pathways involved have been summarized under three crucial aspects: antivascular effects, induction of cell death, and effects on cell movement and metastasis. Most of these effects have been described for CA-4 or its prodrug CA-4P but also for several combretastatin-like compounds.

5.1. Antivascular Effects. *5.1.1. Vascular-Disrupting Activity.* As mentioned before, tubulin-binding VDAs take advantage of the unstable and immature intratumoral vasculature to selectively target tumor blood vessels as opposed to normal vessels. The kinetics of the antivascular effect of CA-4P have been extensively investigated using various methods, including dynamic bioluminescence imaging, intravital microscopy, magnetic resonance imaging, and histology.[24,136−139] Already in 1997, Dark et al.[24] showed that CA-4P induces vascular shutdown at doses less than one-tenth of the maximum tolerated dose. Further studies demonstrated that tumor blood flow was reduced within 1 h and that CA-4P caused the loss of a large proportion of the smallest blood vessels,[136] resulting in a significant reduction in mean vessel radius, as shown later using MRI-based vessel size imaging.[140] However, tumor perfusion and oxygenation status returned to normal after 24 h following a single injection of CA-4P.[141]

Lunt et al.[142] demonstrated that the vascular-disrupting effect of CA-4P dominates the tumor response to CA-4P rather than direct tumor cell cytotoxicity. These authors showed that SW122 human colorectal carcinoma cells resistant to CA-4P in vitro (no inhibition of cell proliferation) were equally sensitive as nonresistant cells to CA-4P in vivo. Moreover, CA-4P induced tumor necrosis, rapid vessel disruption, and blood flow shutdown in xenografts derived from both cell lines.[142]

The molecular and cellular pathways that support the maintenance and stability of the tumor microvasculature are not well-defined. However, important roles have been shown for pericytes, specialized smooth muscle cells that cover and stabilize microvessels, and for various adhesion molecules and integrins that provide survival signals to endothelial cells.[8] As already mentioned, the destabilization of the endothelial cytoskeleton and increase in vascular permeability induced by combretastatins and analogues are thought to contribute to the occlusion of the tumor vasculature, which is immature and abnormal and lacks essential support by pericytes and basement membrane.[8] In theory, increased permeability could cause a transient increase in interstitial fluid pressure, which in turn could induce intratumoral blood vessel collapse. However, there is no experimental evidence to corroborate this hypothesis.[143] Using a ROCK inhibitor, it was shown that activation of Rho/ROCK is crucial for the antivascular effects of CA-4P in tumor-bearing mice.[144] Importantly, CA-4P was found to selectively induce regression of unstable tumor neovessels both in vitro and in mice by inhibiting cellular signaling through vascular endothelial-cadherin (VE-cadherin), a crucial cell-specific junctional molecule.[145] Disruption of the VE-cadherin/β-catenin/Akt signaling pathway also increased endothelial cell permeability, leading to rapid vascular collapse and tumor necrosis. On the other hand, stabilization of VE-cadherin signaling in endothelial cells or enclosure of endothelial cells with smooth muscle cells conferred resistance to CA-4P.[145] These data demonstrate the ability of tubulin-disrupting VDAs to discriminate between normal physiological vessels and unstable intratumoral vessels, a discrimination that is critical for their clinical applicability.

5.1.2. Antiangiogenic Activity. Angiogenesis is a complex multistep process that requires, e.g., the proliferation, migration, and tube formation of endothelial cells. Besides their destructive effect on the existing vasculature, several VDAs, including CA-4 and its analogues[146] and deoxypodophyllotoxin[147] (DPT, the 5-deoxyderivative of compound **6**), a natural product isolated from *Anthriscus sylvestris*, have also been shown to inhibit the formation of new blood vessels. Interestingly, sprout formation and migration were reduced at concentrations that were not cytotoxic to endothelial cells.[148,149] Using the 2-aminothiazole derivative **15**,[149] it was shown that inhibition of angiogenesis and increase in vascular permeability involved the VE-cadherin/β-catenin signaling pathway. It has also been proposed that connective tissue growth factor (CTGF/CCN2), an endogenous antiangiogenic agent, is involved in the antiangiogenic activity of CA-4P.[150] Upregulation of CTGF in microvascular endothelial cells by CA-4P was dependent on ROCK signaling and was increased by MAPK/Erk inhibitors, providing a possible explanation for the improved clinical efficacy of combretastatins when combined with kinase inhibitors.[150]

5.2. CA-4P Induces Endothelial and Tumor Cell Death. Several types of cell death may occur following treatment of cells with tubulin-binding VDAs, including apoptosis, mitotic catastrophe, necrosis, and autophagy, which are executed by distinct and sometimes overlapping pathways.[151]

5.2.1. CA-4P Induces Mitotic Arrest and Mitotic Catastrophe in Endothelial and Tumor Cells. Microtubule-binding agents typically abrogate appropriate spindle formation during mitosis, leading to cell cycle arrest in G2/M phase. Mitotic arrest was demonstrated by elevated levels of cyclin B1 protein and increased cyclin-dependent kinase (cdc2) activity. Sustained cdc2 activity was responsible for metaphase arrest.[152−154] Interestingly, Kanthou et al.[153] showed that CA4P-induced endothelial cell death was restricted to proliferating (mitotic) cells. This may be linked to the fact that failure of cells to proceed through mitosis has been shown

DOI: 10.1021/acs.jmedchem.6b00463
J. Med. Chem. 2016, 59, 8685−8711

to result in mitotic catastrophe, a form of cell death induced by aberrant chromosome segregation during mitosis or DNA damage. This process is thought to protect normal cells with irregular mitosis from becoming aneuploid and potentially oncogenic, as reviewed in Vitale et al.,[155] but it is also induced by several DNA damaging and microtubule-binding compounds. Accordingly, experimental data obtained in a panel of human B-lymphoid tumors indicate that mitotic catastrophe is the primary form of cell death induced by CA-4.[154,156] Mitotic catastrophe has also been reported in various other cell lines treated with combretastatins, such as lung,[157,158] bladder,[152] cervical,[52] and breast cancer cells.[159]

5.2.2. Combretastatins Induce Endothelial and Tumor Cell Apoptosis. Increasing data indicate that mitotic catastrophe may proceed toward other forms of cell death, such as apoptosis (or necrosis, depending on the pathways involved). Two different apoptotic pathways have been described: the intrinsic pathway, which results from mitochondrial damage and subsequent cytochrome c release from the mitochondria, and the extrinsic pathway, which is activated as a result of activation of cell death receptors on the cell surface. Both pathways typically converge on the activation of caspases, cysteine-dependent proteases responsible for the organized disassembly of the cell, as recently reviewed.[160]

Already in 1998, Iyer et al. showed that the cytotoxic effect of CA-4 was mediated by the induction of apoptosis, as characterized by increased caspase-3 activation and internucleosomal DNA fragmentation.[161] Moreover, treatment of acute myeloid leukemias (AMLs) with CA-4P led to disruption of mitochondrial membrane potential and release of proapoptotic mitochondrial membrane proteins, resulting in cell death. This was partially ascribed to caspase activation, although an increase of the intracellular reactive oxygen species (ROS) also contributed to CA-4P-induced cytotoxicity in AML.[162] Also in H460 lung cancer cells treated with CA-4, mitochondrial membrane permeabilization followed by cytochrome c release and caspase activation was observed.[158] These data all point to a predominant mitochondrial involvement (i.e., intrinsic pathway) in combretastatin-mediated apoptosis.

Further investigation of the molecular mediators involved revealed an important role for the Bcl-2 family of proteins. Using knock-down experiments, it was shown that the apoptosis-promoting protein Bim (BH3-only protein belonging to Bcl-2 family), which is sequestered on the microtubule array (type of interface microtubule organization independent of a centrosome), is essential for CA-4-induced cell death in H460 lung cancer cells. It has been proposed that Bim promotes the release of proapoptotic Bax from the prosurvival protein Bcl-2, resulting in increased tumor cell apoptosis.[163] A subsequent study by these authors disclosed an essential role for the tumor-suppressor protein p53 in the mitochondrial accumulation of Bim and resulting apoptotic events in nonsmall cell lung cancer.[164] Additionally, NF-κB and c-Jun N-terminal kinase (JNK) were found to be crucial for the apoptosis-inducing capacity of the CA-4 analogue Brimanin, an N-Me imidazole derivative analogue of **16** with a 3-bromo-3,4-dimethoxyphenyl as ring A in pancreas and breast carcinoma cell lines.[165]

In contrast, several studies using solid as well as leukemia cell lines demonstrated CA-4P-induced cell death independent of caspase activation[153] or poly(ADP-ribose) polymerase (PARP) cleavage,[154] suggesting that apoptosis is not involved or only plays a minor role in cell death induced by CA-4P. Moreover, in vitro studies using a stilbene derivative (the 3,5-dimethoxyphenyl derivative at ring A of 3′-amino-deoxycombretastatin A-4) reported induction of mitotic catastrophe and apoptosis in HCT-116 human colon cancer cells but not in B16/F10 melanoma cells.[151] In summary, despite some reports that show apoptosis-independent cell death induced by combretastatins, the majority of studies demonstrate an involvement of the mitochondrial apoptosis pathway. However, apoptosis induction by combretastatins seems to be context- and cell-dependent and the signaling pathways involved remain ill-defined.

5.3. CA-4P Inhibits Cell Movement and Metastasis. Tubulin-binding VDAs do not only block cell mitosis but also affect endothelial and tumor cell morphology and movement and prevent tumor cell metastasis. Specifically, CA-4 reduced the attachment, migration, and invasiveness of gastric cancer cells by inhibition of the phosphoinositol (PI)3 kinase/AKT survival pathway.[166] CA-4 also inhibited bladder cancer cell migration in vitro.[152] CA-4P has been shown to attenuate gastric tumor metastasis and AKT activation in vivo, suggesting that reduced survival signals contribute to the observed antimetastatic effects.[166] In addition, CA-4P inhibited the circulation of acute myeloid leukemia cells (AMLs) and the extent of perivascular leukemic infiltrates.[162] This effect may be explained by CA-4P-induced downregulation of vascular endothelial adhesion molecule (VCAM)-1 expression on the endothelial cell surface, resulting in reduced interaction of AMLs with blood vessels and subsequent augmented leukemic cell death.[162] Other combretastatin-like compounds also inhibited cell migration and/or metastasis.[149,167,168] In particular, compound **12** reduced lymph node metastasis of LY80 Yoshida sarcoma in mice by shutting down the blood flow even in small metastases. These observations suggest that combretastatin-mediated vascular shutdown not only affects large primary tumors but also micrometastases.[168]

An important role has been attributed to the Rho/ROCK pathway in the CA-4-induced antimigration effect. Rho-associated kinases (ROCK) induce the formation of stress fibers and focal adhesions by phosphorylating the myosin light chain (MLC), leading to actin binding to myosin II and increased contractility as reviewed by Ridley.[169] High levels of Rho/ROCK signaling may further lead to "bleb-driven" cell migration, in addition to the more frequently used "lamellipodium-based" migration.[169] In endothelial cells, CA-4P caused within minutes the phosphorylation of MLC, leading to actinomyosin contractility, assembly of actin stress fibers, and formation of focal adhesions. However, some cells also rapidly acquired a blebbing morphology, which was associated with increased monolayer permeability and decreased cell viability. Cytoskeletal alterations as well as blebbling were abolished by inhibiting the Rho/ROCK pathway or by blocking activation of stress-activated protein kinase-2/p38.[170] In contrast, the extracellular-regulated kinases 1 and 2 (ERK-1/2) were shown to protect against blebbing.[170] Rho activation was also involved in cytoskeleton remodeling induced by other VDAs, including deoxypodophyllotoxin (DPT)[147,171] and the CA-4 analogue brimanin.[165]

In summary, CA-4P-mediated inhibition of cell motility and invasion contributes to the observed antitumor and, in particular, to its antimetastatic activity, and may be the consequence of alterations in microtubule organization and associated signaling pathways and/or reduced expression of adhesion molecules that interfere with tumor cell adhesion to the vasculature.

DOI: 10.1021/acs.jmedchem.6b00463
J. Med. Chem. 2016, 59, 8685−8711

6. MECHANISMS OF RESISTANCE AGAINST CA-4P

The efficacy of VDAs in tumor therapy depends on both the immediate vascular shutdown and the subsequent revascularization and regrowth of the tumor from the remaining viable rim. To optimize anticancer treatment with VDAs, it is imperative to get insights into the process of revascularization and tumor regrowth, as summarized in this section.

6.1. Regrowth from the Remaining Viable Tumor Rim. Using **12**, it was shown that only intratumoral vessels are disrupted after treatment of sarcoma xenografts, whereas the vessels at the tumor−host interface remain unaffected.[172] Thus, tumor cells at the necrotic border may survive because they remain fueled by the vessels at the tumor-host interface. Yao et al.[173] further demonstrated that CA-4P-induced hypoxia in W256 tumor-bearing rats resulted in increased vascular mimicry (VM), a recently discovered form of angiogenesis, in which tumor cells form functional vascular channels without endothelial cell participation.[173]

6.2. Induction of a More Aggressive and Hypoxic Environment. A general consequence of VDA treatment is blood vessel collapse, resulting in reduced blood flow and consequently hypoxia in the central tumor area. The major regulator of neovascularization in tumor tissue is hypoxia inducible factor (HIF)-1α, which is upregulated under hypoxia. This transcription factor induces the expression of various proangiogenic molecules, including cytokines such as vascular endothelial growth factor (VEGF) and stromal cell-derived factor (SDF)-1/CXCL12, proteolytic enzymes (e.g., matrix metalloproteinases (MMPs), and inducible nitric oxide synthase (iNOS). CA-4P was shown to induce widespread hypoxia in both peripheral and central parts of the tumor within 1 h after treatment.[174] However, 24 h post treatment, when most of the tumor had turned necrotic, pathophysiological conditions in the surviving viable rim were returning to normal and hypoxia was restricted to regions bordering the necrotic tumor center.[174] In vitro, CA-4P increased HIF-1α accumulation and VEGF expression under aerobic conditions. The compound also activated NF-κB via the small guanosine triphosphatase RhoA.[175]

As mentioned above, hypoxia was also responsible for vascular mimicry induced by CA-4P in tumors through the HIF-1α-induced EphrinA2/PI3K/MMP signaling pathway, resulting in the regrowth of the damaged tumor.[173] Thus, although originally proposed as a tumor-killing mechanism, deprivation of tumor blood flow by antiangiogenic agents and VDAs may paradoxically select for hypoxia-resistant tumor cells that may present increased angiogenic and metastatic potential.

6.3. Recruitment of Endothelial Progenitor Cells. Circulating endothelial progenitor cells (EPC) are a subtype of stem cells with high proliferative potential that are capable of differentiating into mature endothelial cells. Emerging evidence suggests that these bone marrow-derived cells contribute to vascularization and tumor progression.[176,177] The recruitment of endothelial progenitors from the bone marrow to the peripheral blood and the tumor site is thought to be induced by vascular damage and hypoxia and is regulated predominantly by VEGF/VEGF receptor and SDF-1/CXCL12/CXCR4 pathways.[178,179] These factors are upregulated under hypoxia and activate their respective receptors, which are expressed on the surface of EPCs. Thus, acute systemic mobilization and homing of EPCs to the viable tumor rim could promote tumor regrowth following treatment with a VDA.

The CA-1 prodrug **11** was found to cause a rapid increase in circulating plasma VEGF, SDF-1, and granulocyte colony stimulating factor (G-CSF) levels in mice.[180] Interestingly, G-CSF knockout mice failed to mobilize EPCs or to increase SDF-1 plasma levels, while treatment of tumors in these mice with **11** led to more necrosis compared with tumors treated in wild-type mice, suggesting that G-CSF may be a key player in VDA-induced EPC recruitment and tumor regrowth.[180] Moreover, inhibition of EPC mobilization by antiangiogenic compounds resulted in a reduction in tumor rim size and enhanced VDA antitumor activity, thus providing a mechanistic rationale for the enhanced efficacy of VDAs when combined with antiangiogenic drugs.[181]

6.4. Recruitment of Neutrophils and Tumor-Associated Macrophages. The importance of the tumor microenvironment in tumor progression has been well established during past years. Besides the tumor vasculature, immune cells play an important role in tumor pathology. In particular, neutrophils produce various cytokines and enzymes with pro-angiogenic activity. In addition, pro-angiogenic TIE2-expressing macrophages (TEMs) have been shown to stimulate cell migration and invasion, angiogenesis, and tumor growth.[182] Thus, both cell types may increase tumor malignancy.

CA-4P was shown to induce infiltration of TEMs in murine mammary tumors. Inhibition of TEM recruitment by abrogating the CXCL12/CXCR4 pathway or by genetically depleting TEMs in tumor-bearing mice increased the efficacy of CA-4P treatment, suggesting that TEMs contribute to tumor resistance to VDAs.[183]

CA4P-induced shutdown of tumor blood flow also resulted in a significant increase in neutrophil infiltration into the tumors.[184] Neutrophil activity protected the tumor vasculature against CA4P-induced injury by the production of nitric oxide, a molecule with vasodilation and blood flow increasing capacities.[184] Recently, Bohn et al.[185] added further proof to the importance of neutrophils in combretastatin resistance by demonstrating that neutrophil-depleted mice treated with CA-4P showed increased intratumoral necrosis. These authors also demonstrated that neutrophil recruitment induced by CA-4P in endothelial cells is the result of increased expression of endothelial cell adhesion molecules, which promote neutrophil attachment to the tumor vasculature.[185] Together, these data strongly suggest a role for TEMs and neutrophils in reducing the CA-4P-mediated antitumor effect. Thus, these immune cells may represent a potential target to be addressed in order to improve the clinical efficacy of VDA-based therapies.

6.5. Effects of CA-4P on Autophagy. Autophagy is a catabolic process that facilitates cell survival in conditions of stress by generating energy via lysosomal degradation of cytoplasmic constituents. In the context of cancer, autophagy may thus act as a tumor promotor by supporting survival of starving tumor cells, as recently reviewed.[160]

CA-4P was shown to cause autophagy in adenocarcinoma-derived, but not in fibrosarcoma-containing, tumor xenografts, suggesting a tumor-dependent mechanism of action.[186] Accordingly, inhibition of autophagy by the vacuolar H(+)-ATPase inhibitor Bafilomycin-A1[186] or by pretreatment with autophagy inhibitors (3-methyladenine, 3-MA) or small interfering RNAs against autophagic genes[187] potentiated CA-4-mediated cell death. The enhanced anticancer activity of the combination of CA-4 and 3-MA was further confirmed in the SGC-7901 xenograft tumor model.[187]

DOI: 10.1021/acs.jmedchem.6b00463
J. Med. Chem. 2016, 59, 8685−8711

Using JNK inhibitors, it was shown that the JNK-Bcl-2 pathway is a critical regulator of CA-4-induced autophagy, which attenuates CA-4-induced apoptosis.[187] Taken together, and although recent data indicate that components of the autophagic signaling pathway may promote cell death,[160] autophagy seems to play predominantly a tumor-promoting role in combretastatin-treated tumors. It may be proposed that inhibition of this process, by combination therapy with autophagy inhibitors, may force VDA-treated tumor cells to enter apoptosis.

7. COMBINATION THERAPY

The clinical success of VDAs relies on the elimination of the viable tumor rim that is resistant to these compounds, which can be achieved by combination with radio/chemotherapy or antiangiogenic therapy. However, the intrinsic strength of VDAs to cause rapid vascular shutdown also poses extra problems in that a reduction of intratumoral tumor blood flow and oxygen tension prevents the uptake of other anticancer agents and reduces the efficacy of radiation therapy. Consequently, scheduling, sequence, and timing become crucial when considering combination regimens involving VDAs in order to maximize the therapeutic efficacy.[26,188,189] For an extensive overview of combination therapies involving VDAs, we refer to several excellent reviews that have recently appeared.[25,190] Here, we only highlight some specific concepts that illustrate the possibilities and pitfalls associated with VDA combination therapies.

7.1. Combination with Antiangiogenic Agents. The mechanistic rational for combining VDAs with angiogenesis inhibitors is 2-fold, i.e., antiangiogenic agents may abrogate (i) neovascularization from the remaining vessels in the tumor rim and (ii) mobilization of EPC from the bone marrow, as already indicated in a previous section.[181]

Although angiogenesis involves various mediators and pathways, studies have, until recently, largely focused on the key angiogenic growth factor VEGF. Consequently, clinical VDA combinations have been limited to the evaluation of CA-4 prodrugs with bevacizumab, a clinically approved monoclonal antibody targeting VEGF.[25,190] Recent phase I trials in patients with advanced cancer treated with CA-4P 4 h before administration of bevacizumab showed reduced and sustained vascular permeability and perfusion compared with CA-4P alone.[191]

Despite these promising results, bevacizumab may not be the ideal antiangiogenic agent to combine with VDAs. Accumulating clinical data indicate that this monoclonal antibody affords only limited antitumor activity and causes rapid tumor resistance due to the expression of other angiogenic factors by the tumor.[192,193] As such, combination with already approved receptor tyrosine kinase inhibitors that target several angiogenic factors might provide a better therapeutic benefit.

7.2. Combination with Chemo/Radiation Therapy. Because of limited perfusion in the center of the tumor, chemo- and radiotherapy are less effective in killing cells at the tumor core. Conversely, these therapies are particularly efficient in the well-vascularized VDA-resistant tumor rim. Therefore, the use of combinations of chemo/radiotherapy with VDAs seems a very promising strategy that has progressed to phase II clinical trials. Most of these studies are still ongoing (https://clinicaltrials.gov). However, the already disclosed results have not always been as encouraging as expected. Combination of CA-4P with carboplatin and paclitaxel gave a higher response rate in patients with relapsed ovarian cancer.[194] However, CA-4P did not significantly improve the survival of patients suffering from anaplastic thyroid cancer treated with carboplatin/paclitaxel.[195] Also, addition of **12** to a taxane regime did not improve progression-free survival of patients with metastatic nonsmall cell lung cancer.[196]

Additional studies should provide more insights into these variable data. However, appropriate scheduling of chemo/radiotherapy and VDAs is critical to maximize anticancer efficiency and minimize toxicity of these combinations. Because chemotherapeutic agents and radiotherapy require an adequate blood flow, they should theoretically be administered before VDAs. Indeed, preclinical data demonstrated that irradiation may prevent tumor recurrence in the tumor rim only when given before **12**.[172] Also, cisplatin enhanced tumor killing only when administered before VDAs.[197] Moreover, in a phase I trial involving patients with various tumors refractory to treatment, CA-4P increased carboplatin-associated toxicity when administered 1 h after the chemotherapeutic agent. Interestingly, bone marrow toxicity could be avoided when both compounds were administered on consecutive days.[198] Also, the combination of paclitaxel and VDAs should be carefully monitored. Martinelli et al.[189] reported that treatment of mice bearing breast cancer with paclitaxel followed by the VDA **7**, a prodrug of *N*-acetylcolchinol, did not result in a beneficial outcome, probably because of a protective effect of paclitaxel against the vascular damage induced by **7**. By contrast, improved antitumor efficacy was observed when **7** was administered before paclitaxel. Thus, scheduling may be critical in the design of these combination approaches.

8. CONCLUSIONS AND PERSPECTIVES

Tubulin-depolymerizing agents acting at the colchicine site have been vastly re-explored in the last 20 years, mostly due to their vascular disrupting properties in the tumor environment. From a chemical point of view, compounds binding at the colchicine site are low molecular weight compounds whose synthesis, in most cases, can be accomplished by standard synthetic methods, which has allowed the testing of large families of compounds and the establishment of well-defined SAR. Using the structure of CA-4 as inspiration, there are now compounds for which chemical instability is not an issue but solubility is still a limitation that is mostly overcome by the derivatization as prodrugs. As mentioned throughout this Perspective, several prodrugs of combretastatin derivatives are being evaluated in clinical trials. There are other compounds, whose structure is not inspired by CA-4, for which oral bioavailability has been accomplished, and several of them are being evaluated in the clinic as well. None of them have yet been approved.

In the last four years, making use of stathmin or other MAPs, the structure of $\alpha\beta$-tubulin complexed with a wide variety of ligands has been solved, shedding light into the detailed atomic features of their binding in the so-called colchicine-binding domain. The higher resolution of these complexes compared to the early examples in 2004 of DAMA−colchicine or podophyllotoxin tubulin-cocrystals have also revealed unknown features of the tubulin structure. Indeed, the insights obtained with these very recent complexes may lead to a reevaluation of the binding mode previously proposed for some ligands based on docking studies. As an example, the binding mode predicted for plinabulin by molecular modeling[86] does not correlate with the interactions observed when the complex of plinabulin with

DOI: 10.1021/acs.jmedchem.6b00463
J. Med. Chem. 2016, 59, 8685−8711

$\alpha\beta$-tubulin was very recently solved.[88] The detailed information now available about the colchicine domain and the binding mode of the different ligands will facilitate a more accurate application of the molecular modeling tools to design new colchicine-domain ligands. Moreover, recent progress on the different conformations of the $\alpha\beta$-tubulin dimer and the activities of key proteins that regulate microtubule dynamics[122,199] may offer new possibilities for therapeutic intervention.

From a biological point of view, and using CA-4 as a prototype, it is becoming clear that microtubule depolymerization in endothelial cells leads to distinct responses affecting chromosome organization, cell morphology and permeability, and cell death. Each of these processes involves several biological pathways that may be targeted by CA-4. Interestingly, even a very close analogue of CA-4, CA-1, exerts a more toxic effect than CA-4 due to the formation of a reactive quinone intermediate. This illustrates the difficulties in predicting the contribution of these different pathways to the antivascular and antitumor activity of CA-4 analogues.

As has also been shown, P-glycoprotein or βIII tubulin overexpression is not relevant for resistance among these compounds. However, rapid tumor recurrence after monotherapy with these compounds occurs through the intrinsic resistance of more stabilized vessels at the tumor border. To surmount these limitations, VDAs are typically administered in combination with therapies that specifically target this viable tumor rim, such as radio- and chemotherapy. Relevant to this point, it should be mentioned that recent progress in understanding the biological actions of VDAs has led to potentially new combination therapies. So far, preclinical studies already demonstrated improved antitumor activity when combretastatins were combined with inhibitors of nitric oxide synthase,[200] autophagy,[187] or the recently discovered mediator of vascular disruption RhoJ,[201] an endothelial-enriched Rho GTPase. In vitro studies further indicated that inhibitors of various intracellular kinases, such as p38 MAPK[202] and JNK,[187] may increase CA-4 anticancer efficacy. Also, neutrophils and TEMs may represent a potential target for improving the clinical efficacy of VDA-based therapies.[183,185] Clinically, combinations assayed so far have been limited to CA-4 prodrugs as VDA, but other VDAs, such as the more active compound CA-1P, or VDAs with a structure that is not related to combretastatins, should be included as well.

Finally, new delivery systems such as nanoparticles or nanocarriers are being explored for selective delivery of CA-4 and its prodrug CA-4P and also for combination therapy. Moreover, VDAs might be used to prime the host environment to become receptive to a second (therapeutic or diagnostic) agent in the so-called environment-primed nanosystems.[203] For example, ombrabulin selectively increases the expression of p32 (a stress-related protein) on the surface of tumor cells, and this has been used to recruit nanoparticles decorated with p32-targeting peptides in the tumor environment.[204] This field will certainly offer interesting perspectives for the future.

AUTHOR INFORMATION

Corresponding Author

*Phone: 34 91 2587516. Fax: 34 91 5644853. E-mail: mjperez@iqm.csic.es.

Notes

The authors declare the following competing financial interest(s): Mara-Dolores Canela is currently working at Teva Pharmaceuticals as Medical Advisor.

Biographies

María-Jesús Pérez-Pérez is Research Professor at the Medicinal Chemistry Institute (IQM-CSIC) (Madrid, Spain). She studied Pharmacy at Universidad de Navarra and received her Ph.D. from Universidad Complutense (Madrid). She stayed as a postdoc for more than two years at Rega Institute (KU Leuven, Belgium) and got a tenured position at CSIC in 1995. She has been director of the IQM-CSIC for four years (2011−2015). Her research work has been linked to selective inhibitors against therapeutically relevant nucleoside processing enzymes (thymidine phosphorylase, nucleoside kinases, etc.) as well to the identification and optimization of antivirals, particularly against HIV, enterovirus, or alphavirus. Her currently active areas of research involve antivascular strategies in the antitumoral field and novel chemical entities against (re)-emerging viruses.

Eva-María Priego received her degree in Chemistry at the Universidad Complutense de Madrid. After enjoying a postdoctoral position with Prof. Sir Tom L. Blundell in the Crystallography and Bioinformatics Unit at the Department of Biochemistry at the University of Cambridge, she returned in 2007 to the Instituto de Química Médica with a CSIC contract from the I3P programme, and since 2009 as Tenured Scientist. Her research interests are in the areas of computer-aided drug design, homology modeling, docking, molecular dynamic simulations of biomolecular systems, and virtual screening, and she is currently focused on the development of new antivascular agents.

Oskía Bueno received her degree in Chemistry at University of Navarra in 2008 and performed an internship during three months in the area of Neurosciences in the Center for Applied Medical Research (University of Navarra). In 2010, she received a Master's degree in Green Chemistry at the Public University of Navarra, being involved in a project at the Department of Applied Chemistry. In 2011, she joined the Medicinal Chemistry Institute (IQM-CSIC) in Madrid, working at the instrumental analysis unit. Since 2013, she is a predoctoral student on a project concerning antivascular strategies against tumor growth under the supervision of Prof. M.-J. Pérez-Pérez and Dr. E. M. Priego. Her research interests concern the design, synthesis, and biological evaluation of new tubulin binding agents with vascular disrupting capacity.

Maria Solange Martins graduated as Bachelor in Biology at the Faculty of Sciences of the University of Lisbon (FCUL, Portugal) in 2012. After an Erasmus program at the Aarhus University (Denmark), she returned to FCUL, where she acquired her Master's degree in Molecular Biology and Genetics in 2014. Solange is currently a Ph.D. student at the Rega Institute (Laboratory of Virology and Chemotherapy, KU Leuven, Belgium) under the supervision of Prof. Sandra Liekens, focusing on the characterization of vascular-disrupting agents.

María-Dolores Canela received her degree in Pharmacy in 2008 by the University of Seville and a Master's degree in Clinical Trials in 2011 by the same university. She got the Pharmacy's Extraordinary Award for the Best Student Record and National Education Award in Pharmacy's degree. After two years working at the Spanish National Centre for Biotechnology (CNB-CSIC), she got a Postgraduate degree in Immunology. In September 2010, and through a JAE-Pre contract, she joined the IQM-CSIC to perform her thesis. She defended her Ph.D. thesis in July 2014, under the supervision of Dr. E.-M. Priego and Prof. M.-J. Pérez-Pérez, focused on the discovery, synthesis, and

DOI: 10.1021/acs.jmedchem.6b00463
J. Med. Chem. 2016, 59, 8685−8711

evaluation of novel tumor vascular disrupting agents. She is currently working at Teva Pharmaceuticals as Medical Advisor.

Sandra Liekens graduated as Bio-Engineer in 1994 at the University of Leuven, Belgium. She obtained her Ph.D. degree (2000) in Applied Biological Sciences at the Rega Institute (Laboratory of Virology and Chemotherapy, KU Leuven, Belgium) on the inhibition of vascular tumor growth by antiangiogenic and apoptosis-inducing agents. After a postdoctoral stay at the New York University (laboratory of Prof. Rifkin), she returned to Leuven where she is currently holding a position of professor at the Rega Institute. Her research is focused on the study of endothelial cell activation by flaviviruses and the characterization of antiangiogenic and vascular-targeting agents.

■ ACKNOWLEDGMENTS

Due to the amount of original research articles and reviews on this subject, we were unable to cite all of them; any omissions were unintentional. Author's research in this subject has been financed by the Spanish Ministerio de Economía y Competitividad (SAF2012-39760-C02-01 and SAF2015-64629-C2-1-R (MINECO-FEDER) to M.-J.P.-P. and E.-M.P.) and Comunidad de Madrid (BIPEDD2; ref P2010/BMD-2457). S.L. and M.-J.P.-P. acknowledge networking contribution by COST Action CM1407 "Challenging organic synthesis inspired by nature-from natural products chemistry to drug discovery". M.-D.C. thanks the Fondo Social Europeo (FSE) and the JAE Predoc Programme for a predoctoral fellowship.

■ ABBREVIATIONS USED

2-ME, 2-methoxyestradiol; 3-MA, 3-methyladenine; AML, acute myeloid leukemias; CA-1, combretastatin A-1; CA-2, combretastatin A-2; CA-4, combretastatin A-4; CA-4P, the phosphate prodrug of CA-4; CDDP-NPs, *cis*-diaminedichloroplatinum loaded nanoparticles; CDL, colchicine-domain ligand; CTGF/CCN2, connective tissue growth factor; DAMA−colchicine, *N*-deacetyl-*N*-(2-mercaptoacetyl)-colchicine; DMXAA, 5,6-dimethylxanthenone-4-acetic acid; DPT, deoxypodophyllotoxin; EBI, *N*,*N*′-ethylene-bis-(iodoacetamide); EGFR, epidermal growth factor receptor; EPC, endothelial progenitor cells; ERK-1/2, extracellular-regulated kinases 1 and 2; FAA, 8-flavon acetic acid; G-CSF, granulocyte colony stimulating factor; (HIF)-1α, hypoxia inducible factor 1α; HTS, high-throughput screening; iNOS, inducible nitric oxide synthase; JNK, c-Jun N-terminal kinase; MAP, microtubule associated protein; MLC, myosin light chain; MMP, matrix metalloproteinase; MRI, magnetic resonance imaging; NF-κB, nuclear factor kB; NSCLC, nonsmall cell lung cancer; PARP, poly(ADP-ribose) polymerase; PDGFR-β, platelet-derived growth factor receptor β; RB3-SLD, stathmin-like domain of the neural protein RB3; ROCK, Rho-associated kinase; ROS, reactive oxygen species; SDF-1, stromal cell-derived factor; SIFt, structural interaction fingerprints; T2RB3, two tubulin heterodimers−RB3 complex; TEM, TIE2-expressing macrophages; TNF-α, tumor necrosis factor-α; TTL, tubulin tyrosine ligase; (VCAM)-1, vascular endothelial adhesion molecule; VDA, vascular disrupting agent; VE-cadherin, vascular endothelial-cadherin; VEGFR-2, vascular endothelial growth factor receptor-2; VM, vascular mimicry

■ REFERENCES

(1) Siemann, D. W.; Bibby, M. C.; Dark, G. G.; Dicker, A. P.; Eskens, F. A. L. M.; Horsman, M. R.; Marmé, D.; LoRusso, P. M. Differentiation and definition of vascular-targeted therapies. *Clin. Cancer Res.* **2005**, *11*, 416−420.
(2) Tozer, G. M.; Kanthou, C.; Baguley, B. C. Disrupting tumour blood vessels. *Nat. Rev. Cancer* **2005**, *5*, 423−435.
(3) Kanthou, C.; Tozer, G. M. Selective destruction of the tumour vasculature by targeting the endothelial cytoskeleton. *Drug Discovery Today: Ther. Strategies* **2007**, *4*, 237−243.
(4) Potente, M.; Gerhardt, H.; Carmeliet, P. Basic and therapeutic aspects of angiogenesis. *Cell* **2011**, *146*, 873−887.
(5) Carmeliet, P. Angiogenesis in life, disease and medicine. *Nature* **2005**, *438*, 932−936.
(6) El-Kenawi, A. E.; El-Remessy, A. B. Angiogenesis inhibitors in cancer therapy: mechanistic perspective on classification and treatment rationales. *Br. J. Pharmacol.* **2013**, *170*, 712−729.
(7) Vasudev, N. S.; Reynolds, A. R. Anti-angiogenic therapy for cancer: current progress, unresolved questions and future directions. *Angiogenesis* **2014**, *17*, 471−494.
(8) Siemann, D. W. The unique characteristics of tumor vasculature and preclinical evidence for its selective disruption by tumor-vascular disrupting agents. *Cancer Treat. Rev.* **2011**, *37*, 63−74.
(9) Siemann, D. W.; Horsman, M. R. Modulation of the tumor vasculature and oxygenation to improve therapy. *Pharmacol. Ther.* **2015**, *153*, 107−124.
(10) Kanthou, C.; Tozer, G. M. Microtubule depolymerizing vascular disrupting agents: novel therapeutic agents for oncology and other pathologies. *Int. J. Exp. Pathol.* **2009**, *90*, 284−294.
(11) Thorpe, P. E. Vascular targeting agents as cancer therapeutics. *Clin. Cancer Res.* **2004**, *10*, 415−427.
(12) Gaya, A. M.; Rustin, G. J. S. Vascular disrupting agents: a new class of drug in cancer therapy. *Clin. Oncol.* **2005**, *17*, 277−290.
(13) Lara, P. N.; Douillard, J. Y.; Nakagawa, K.; von Pawel, J. v.; McKeage, M. J.; Albert, I.; Losonczy, G.; Reck, M.; Heo, D.-S.; Fan, X.; Fandi, A.; Scagliotti, G. Randomized phase III placebo-controlled trial of carboplatin and paclitaxel with or without the vascular disrupting agent vadimezan (ASA404) in advanced non-small-cell lung cancer. *J. Clin. Oncol.* **2011**, *29*, 2965−2971.
(14) LoRusso, P. M.; Boerner, S. A.; Hunsberger, S. Clinical development of vascular disrupting agents: what lessons can we learn from ASA404? *J. Clin. Oncol.* **2011**, *29*, 2952−2955.
(15) Kretzschmann, V.; Fürst, R. Plant-derived vascular disrupting agents: compounds, actions, and clinical trials. *Phytochem. Rev.* **2014**, *13*, 191−206.
(16) Risinger, A. L.; Giles, F. J.; Mooberry, S. L. Microtubule dynamics as a target in oncology. *Cancer Treat. Rev.* **2009**, *35*, 255−261.
(17) Shelanski, M. L.; Taylor, E. W. Properties of the protein subunit of central-pair and outer-doublet microtubules of sea urchin flagella. *J. Cell Biol.* **1968**, *38*, 304−315.
(18) Ravelli, R. B. G.; Gigant, B.; Curmi, P. A.; Jourdain, I.; Lachkar, S.; Sobel, A.; Knossow, M. Insight into tubulin regulation from a complex with colchicine and a stathmin-like domain. *Nature* **2004**, *428*, 198−202.
(19) Bhattacharyya, B.; Panda, D.; Gupta, S.; Banerjee, M. Antimitotic activity of colchicine and the structural basis for its interaction with tubulin. *Med. Res. Rev.* **2008**, *28*, 155−183.
(20) Leung, Y. Y.; Hui, L. L. Y.; Kraus, V. B. Colchicine-Update on mechanisms of action and therapeutic uses. *Semin. Arthritis Rheum.* **2015**, *45*, 341−350.
(21) Pettit, G. R.; Cragg, G. M.; Singh, S. B. Antineoplastic agents 122. Constituents of *Combretum caffrum*. *J. Nat. Prod.* **1987**, *50*, 386−391.
(22) Pettit, G. R.; Temple, C. J.; Narayanan, V. L.; Varma, R.; Simpson, M. J.; Boyd, M. R.; Rener, G. A.; Bansal, N. Antineoplastic agents 322. Synthesis of combretastatin A-4 prodrugs. *Anti-Cancer Drug Des.* **1995**, *10*, 299−309.
(23) Lin, C. M.; Ho, H. H.; Pettit, G. R.; Hamel, E. Antimitotic natural products combretastatin A-4 and combretastatin A-2: Studies on the mechanism of their inhibition of the binding of colchicine to tubulin. *Biochemistry* **1989**, *28*, 6984−6991.

DOI: 10.1021/acs.jmedchem.6b00463
J. Med. Chem. 2016, 59, 8685−8711

(24) Dark, G. G.; Hill, S. A.; Prise, V. E.; Tozer, G. M.; Pettit, G. R.; Chaplin, D. J. Combretastatin A-4, an agent that displays potent and selective toxicity toward tumor vasculature. *Cancer Res.* **1997**, *57*, 1829−1834.
(25) Greene, L. M.; Meegan, M. J.; Zisterer, D. M. Combretastatins: more than just vascular targeting agents? *J. Pharmacol. Exp. Ther.* **2015**, *355*, 212−227.
(26) Mita, M. M.; Sargsyan, L.; Mita, A. C.; Spear, M. Vascular-disrupting agents in oncology. *Expert Opin. Invest. Drugs* **2013**, *22*, 317−328.
(27) Porcu, E.; Bortolozzi, R.; Basso, G.; Viola, G. Recent advances in vascular disrupting agents in cancer therapy. *Future Med. Chem.* **2014**, *6*, 1485−1498.
(28) Ji, Y. T.; Liu, Y. N.; Liu, Z. P. Tubulin colchicine binding site inhibitors as vascular disrupting agents in clinical developments. *Curr. Med. Chem.* **2015**, *22*, 1348−1360.
(29) Barbier, P.; Tsvetkov, P. O.; Breuzard, G.; Devred, F. Deciphering the molecular mechanisms of anti-tubulin plant derived drugs. *Phytochem. Rev.* **2014**, *13*, 157−169.
(30) Tsvetkov, P. O.; Barbier, P.; Breuzard, G.; Peyrot, V.; Devred, F. Microtubule-associated proteins and tubulin interaction by isothermal titration calorimetry. In *Methods in Cell Biology*; John, J. C., Leslie, W., Eds.; Academic Press: New York, 2013; Vol. *115*, pp 283−302.
(31) Fortin, S.; Lacroix, J.; Côté, M. F.; Moreau, E.; Petitclerc, É.; C.-Gaudreault, R. Quick and simple detection technique to assess the binding of antimicrotubule agents to the colchicine-binding site. *Biol. Proced. Online* **2010**, *12*, 113−117.
(32) Canela, M. D.; Pérez-Pérez, M. J.; Noppen, S.; Sáez-Calvo, G.; Díaz, J. F.; Camarasa, M. J.; Liekens, S.; Priego, E. M. Novel colchicine-site binders with a cyclohexanedione scaffold identified through a ligand-based virtual screening approach. *J. Med. Chem.* **2014**, *57*, 3924−3938.
(33) Canela, M. D.; Bueno, O.; Noppen, S.; Sáez Calvo, G.; Estévez Gallego, J.; Díaz, J. F.; Camarasa, M. J.; Liekens, S.; Pérez-Pérez, M. J.; Priego, E. M. Targeting the colchicine site in tubulin through cyclohexanedione derivatives. *RSC Adv.* **2016**, *6*, 19492−19506.
(34) Hadimani, M. B.; MacDonough, M. T.; Ghatak, A.; Strecker, T. E.; Lopez, R.; Sriram, M.; Nguyen, B. L.; Hall, J. J.; Kessler, R. J.; Shirali, A. R.; Liu, L.; Garner, C. M.; Pettit, G. R.; Hamel, E.; Chaplin, D. J.; Mason, R. P.; Trawick, M. L.; Pinney, K. G. Synthesis of a 2-aryl-3-aroyl indole salt (OXi8007) resembling Combretastatin A-4 with application as a vascular disrupting agent. *J. Nat. Prod.* **2013**, *76*, 1668−1678.
(35) Tron, G. C.; Pirali, T.; Sorba, G.; Pagliai, F.; Busacca, S.; Genazzani, A. A. Medicinal chemistry of combretastatin A4: present and future directions. *J. Med. Chem.* **2006**, *49*, 3033−3044.
(36) Lu, Y.; Chen, J.; Xiao, M.; Li, W.; Miller, D. D. An overview of tubulin inhibitors that interact with the colchicine binding site. *Pharm. Res.* **2012**, *29*, 2943−2971.
(37) Shan, Y. S.; Zhang, J.; Liu, Z.; Wang, M.; Dong, Y. Developments of combretastatin A-4 derivatives as anticancer agents. *Curr. Med. Chem.* **2011**, *18*, 523−538.
(38) Marrelli, M.; Conforti, F.; Statti, G. A.; Cachet, X.; Michel, S.; Tillequin, F.; Menichini, F. Biological potential and structure-activity relationships of most recently developed vascular disrupting agents: An overview of new derivatives of natural combretastatin A-4. *Curr. Med. Chem.* **2011**, *18*, 3035−3081.
(39) Patil, P. O.; Patil, A. G.; Rane, R. A.; Patil, P. C.; Deshmukh, P. K.; Bari, S. B.; Patil, D. A.; Naphade, S. S. Recent advancement in discovery and development of natural product combretastatin-inspired anticancer agents. *Anti-Cancer Agents Med. Chem.* **2015**, *15*, 955−969.
(40) Rajak, H.; Kumar Dewangan, P.; Patel, V.; Kumar Jain, D.; Singh, A.; Veerasamy, R.; Chander Sharma, P.; Dixit, A. Design of combretastatin A-4 analogs as tubulin targeted vascular disrupting agent with special emphasis on their cis-restricted isomers. *Curr. Pharm. Des.* **2013**, *19*, 1923−1955.
(41) Kaur, R.; Kaur, G.; Gill, R. K.; Soni, R.; Bariwal, J. Recent developments in tubulin polymerization inhibitors: An overview. *Eur. J. Med. Chem.* **2014**, *87*, 89−124.
(42) Álvarez, R.; Medarde, M.; Peláez, R. New ligands of the tubulin colchicine site based on X-ray structures. *Curr. Top. Med. Chem.* **2014**, *14*, 2231−2252.
(43) Massarotti, A.; Coluccia, A.; Silvestri, R.; Sorba, G.; Brancale, A. The tubulin colchicine domain: a molecular modeling perspective. *ChemMedChem* **2012**, *7*, 33−42.
(44) Hartley, R. M.; Peng, J.; Fest, G. A.; Dakshanamurthy, S.; Frantz, D. E.; Brown, M. L.; Mooberry, S. L. Polygamain, a new microtubule depolymerizing agent that occupies a unique pharmacophore in the colchicine site. *Mol. Pharmacol.* **2012**, *81*, 431−439.
(45) Jordan, M. A.; Wilson, L. Microtubules as target for anticancer drugs. *Nat. Rev. Cancer* **2004**, *4*, 253−265.
(46) Pettit, G. R.; Singh, S. B.; Boyd, M. R.; Hamel, E.; Pettit, R. K.; Schmidt, J. M.; Hogan, F. Antineoplastic agents. 291. Isolation and synthesis of combretastatins A-4, A-5, and A-6. *J. Med. Chem.* **1995**, *38*, 1666−1672.
(47) Pettit, G. R.; Rhodes, M. R.; Herald, D. L.; Chaplin, D. J.; Stratford, M. R. L.; Hamel, E.; Pettit, R. K.; Chapuis, J. C.; Oliva, D. Antineoplastic agents 393. Synthesis of the trans-isomer of combretastatin A-4 prodrug. *Anti-Cancer Drug Des.* **1998**, *13*, 981−993.
(48) Pettit, G. R.; Lippert, J. W. Antineoplastic agents 429. Syntheses of the combretastatin A-1 and combretastatin B-1 prodrugs. *Anti-Cancer Drug Des.* **2000**, *15*, 203−216.
(49) Ohsumi, K.; Nakagawa, R.; Fukuda, Y.; Hatanaka, T.; Morinaga, Y.; Nihei, Y.; Ohishi, K.; Suga, Y.; Akiyama, Y.; Tsuji, T. Novel combretastatin analogues effective against murine solid tumors: Design and structure−activity relationships. *J. Med. Chem.* **1998**, *41*, 3022−3032.
(50) Folkes, L. K.; Christlieb, M.; Madej, E.; Stratford, M. R. L.; Wardman, P. Oxidative metabolism of combretastatin A-1 produces quinone intermediates with the potential to bind to nucleophiles and to enhance oxidative stress via free radicals. *Chem. Res. Toxicol.* **2007**, *20*, 1885−1894.
(51) Ohsumi, K.; Hatanaka, T.; Fujita, K.; Nakagawa, R.; Fukuda, Y.; Nihei, Y.; Suga, Y.; Morinaga, Y.; Akiyama, Y.; Tsuji, T. Syntheses and antitumor activity of cis-restricted combretastatins: 5-Membered heterocyclic analogues. *Bioorg. Med. Chem. Lett.* **1998**, *8*, 3153−3158.
(52) Romagnoli, R.; Baraldi, P. G.; Brancale, A.; Ricci, A.; Hamel, E.; Bortolozzi, R.; Basso, G.; Viola, G. Convergent synthesis and biological evaluation of 2-amino-4-(3′,4′,5′-trimethoxyphenyl)-5-aryl thiazoles as microtubule targeting agents. *J. Med. Chem.* **2011**, *54*, 5144−5153.
(53) Wang, L.; Woods, K. W.; Li, Q.; Barr, K. J.; McCroskey, R. W.; Hannick, S. M.; Gherke, L.; Credo, R. B.; Hui, Y.-H.; Marsh, K.; Warner, R.; Lee, J. Y.; Zielinski-Mozng, N.; Frost, D.; Rosenberg, S. H.; Sham, H. L. Potent, orally active heterocycle-based combretastatin A-4 analogues: synthesis, structure−activity relationship, pharmacokinetics, and in vivo antitumor activity evaluation. *J. Med. Chem.* **2002**, *45*, 1697−1711.
(54) Zhang, Q.; Peng, Y.; Wang, X. I.; Keenan, S. M.; Arora, S.; Welsh, W. J. Highly potent triazole-based tubulin polymerization inhibitors. *J. Med. Chem.* **2007**, *50*, 749−754.
(55) Arora, S.; Wang, X. I.; Keenan, S. M.; Andaya, C.; Zhang, Q.; Peng, Y.; Welsh, W. J. Novel microtubule polymerization inhibitor with potent antiproliferative and antitumor activity. *Cancer Res.* **2009**, *69*, 1910−1915.
(56) Sun, L.; Vasilevich, N. I.; Fuselier, J. A.; Hocart, S. J.; Coy, D. H. Examination of the 1,4-disubstituted azetidinone ring system as a template for combretastatin A-4 conformationally restricted analogue design. *Bioorg. Med. Chem. Lett.* **2004**, *14*, 2041−2046.
(57) O'Boyle, N. M.; Carr, M.; Greene, L. M.; Bergin, O.; Nathwani, S. M.; McCabe, T.; Lloyd, D. G.; Zisterer, D. M.; Meegan, M. J. Synthesis and evaluation of azetidinone analogues of combretastatin A-4 as tubulin targeting agents. *J. Med. Chem.* **2010**, *53*, 8569−8584.
(58) Greene, T. F.; Wang, S.; Greene, L. M.; Nathwani, S. M.; Pollock, J. K.; Malebari, A. M.; McCabe, T.; Twamley, B.; O'Boyle, N. M.; Zisterer, D. M.; Meegan, M. J. Synthesis and biochemical evaluation of 3-phenoxy-1,4-diarylazetidin-2-ones as tubulin-targeting antitumor agents. *J. Med. Chem.* **2016**, *59*, 90−113.

DOI: 10.1021/acs.jmedchem.6b00463
J. Med. Chem. 2016, 59, 8685−8711

(59) Jiang, J.; Zheng, C.; Zhu, K.; Liu, J.; Sun, N.; Wang, C.; Jiang, H.; Zhu, J.; Luo, C.; Zhou, Y. Quantum chemistry calculation-aided structural optimization of combretastatin A-4-like tubulin polymerization inhibitors: improved stability and biological activity. *J. Med. Chem.* **2015**, *58*, 2538−2546.
(60) Pettit, G. R.; Toki, B.; Herald, D. L.; Verdier-Pinard, P.; Boyd, M. R.; Hamel, E.; Pettit, R. K. Antineoplastic agents. 379. Synthesis of phenstatin phosphate1a. *J. Med. Chem.* **1998**, *41*, 1688−1695.
(61) Lee, J.; Kim, S. J.; Choi, H.; Kim, Y. H.; Lim, I. T.; Yang, H.-m.; Lee, C. S.; Kang, H. R.; Ahn, S. K.; Moon, S. K.; Kim, D.-H.; Lee, S.; Choi, N. S.; Lee, K. J. Identification of CKD-516: a potent tubulin polymerization inhibitor with marked antitumor activity against murine and human solid tumors. *J. Med. Chem.* **2010**, *53*, 6337−6354.
(62) Oh, D. Y.; Kim, T. M.; Han, S. W.; Shin, D. Y.; Lee, Y. G.; Lee, K. W.; Kim, J. H.; Kim, T. Y.; Jang, I. J.; Lee, J. S.; Bang, Y. J. Phase I study of CKD-516, a novel vascular disrupting agent, in patients with advanced solid tumors. *Cancer Res. Treat.* **2016**, *48*, 28−36.
(63) Kuo, C. C.; Hsieh, H. P.; Pan, W. Y.; Chen, C. P.; Liou, J. P.; Lee, S. J.; Chang, Y. L.; Chen, L. T.; Chen, C. T.; Chang, J. Y. BPR0L075, a novel synthetic indole compound with antimitotic activity in human cancer cells, exerts effective antitumoral activity in vivo. *Cancer Res.* **2004**, *64*, 4621−4628.
(64) Tung, Y. S.; Coumar, M. S.; Wu, Y. S.; Shiao, H. Y.; Chang, J. Y.; Liou, J. P.; Shukla, P.; Chang, C. W.; Chang, C. Y.; Kuo, C. C.; Yeh, T. K.; Lin, C. Y.; Wu, J. S.; Wu, S. Y.; Liao, C. C.; Hsieh, H. P. Scaffold-hopping strategy: synthesis and biological evaluation of 5,6-fused bicyclic heteroaromatics to identify orally bioavailable anticancer agents. *J. Med. Chem.* **2011**, *54*, 3076−3080.
(65) Flynn, B. L.; Gill, G. S.; Grobelny, D. W.; Chaplin, J. H.; Paul, D.; Leske, A. F.; Lavranos, T. C.; Chalmers, D. K.; Charman, S. A.; Kostewicz, E.; Shackleford, D. M.; Morizzi, J.; Hamel, E.; Jung, M. K.; Kremmidiotis, G. Discovery of 7-hydroxy-6-methoxy-2-methyl-3-(3,4,5-trimethoxybenzoyl)benzo[b]furan (BNC105), a tubulin polymerization inhibitor with potent antiproliferative and tumor vascular disrupting properties. *J. Med. Chem.* **2011**, *54*, 6014−6027.
(66) Kremmidiotis, G.; Leske, A. F.; Lavranos, T. C.; Beaumont, D.; Gasic, J.; Hall, A.; O'Callaghan, M.; Matthews, C. A.; Flynn, B. BNC105: A novel tubulin polymerization inhibitor that selectively disrupts tumor vasculature and displays single-agent antitumor efficacy. *Mol. Cancer Ther.* **2010**, *9*, 1562−1573.
(67) Nien, C. Y.; Chen, Y. C.; Kuo, C. C.; Hsieh, H. P.; Chang, C. Y.; Wu, J. S.; Wu, S. Y.; Liou, J. P.; Chang, J. Y. 5-Amino-2-aroylquinolines as highly potent tubulin polymerization inhibitors. *J. Med. Chem.* **2010**, *53*, 2309−2313.
(68) Wen, Z.; Xu, J.; Wang, Z.; Qi, H.; Xu, Q.; Bai, Z.; Zhang, Q.; Bao, K.; Wu, Y.; Zhang, W. 3-(3,4,5-Trimethoxyphenylselenyl)-1H-indoles and their selenoxides as combretastatin A-4 analogs: Microwave-assisted synthesis and biological evaluation. *Eur. J. Med. Chem.* **2015**, *90*, 184−194.
(69) Romagnoli, R.; Baraldi, P. G.; Salvador, M. K.; Prencipe, F.; Lopez-Cara, C.; Schiaffino Ortega, S.; Brancale, A.; Hamel, E.; Castagliuolo, I.; Mitola, S.; Ronca, R.; Bortolozzi, R.; Porcù, E.; Basso, G.; Viola, G. Design, synthesis, in vitro, and in vivo anticancer and antiangiogenic activity of novel 3-arylaminobenzofuran derivatives targeting the colchicine site on tubulin. *J. Med. Chem.* **2015**, *58*, 3209−3222.
(70) La Regina, G.; Bai, R.; Coluccia, A.; Famiglini, V.; Pelliccia, S.; Passacantilli, S.; Mazzoccoli, C.; Ruggieri, V.; Verrico, A.; Miele, A.; Monti, L.; Nalli, M.; Alfonsi, R.; Di Marcotullio, L.; Gulino, A.; Ricci, B.; Soriani, A.; Santoni, A.; Caraglia, M.; Porto, S.; Da Pozzo, E.; Martini, C.; Brancale, A.; Marinelli, L.; Novellino, E.; Vultaggio, S.; Varasi, M.; Mercurio, C.; Bigogno, C.; Dondio, G.; Hamel, E.; Lavia, P.; Silvestri, R. New indole tubulin assembly inhibitors cause stable arrest of mitotic progression, enhanced stimulation of natural killer cell cytotoxic activity, and repression of Hedgehog-dependent cancer. *J. Med. Chem.* **2015**, *58*, 5789−5807.
(71) Álvarez, R.; Puebla, P.; Díaz, J. F.; Bento, A. C.; García-Navas, R.; de la Iglesia-Vicente, J.; Mollinedo, F.; Andreu, J. M.; Medarde, M.; Peláez, R. Endowing indole-based tubulin inhibitors with an anchor for derivatization: highly potent 3-substituted indolephenstatins and indoleisocombretastatins. *J. Med. Chem.* **2013**, *56*, 2813−2827.
(72) Lu, Y.; Li, C. M.; Wang, Z.; Chen, J.; Mohler, M. L.; Li, W.; Dalton, J. T.; Miller, D. D. Design, synthesis, and SAR studies of 4-substituted methoxylbenzoyl-aryl- thiazoles analogues as potent and orally bioavailable anticancer agents. *J. Med. Chem.* **2011**, *54*, 4678−4693.
(73) La Regina, G.; Bai, R.; Coluccia, A.; Famiglini, V.; Pelliccia, S.; Passacantilli, S.; Mazzoccoli, C.; Ruggieri, V.; Sisinni, L.; Bolognesi, A.; Rensen, W. M.; Miele, A.; Nalli, M.; Alfonsi, R.; Di Marcotullio, L.; Gulino, A.; Brancale, A.; Novellino, E.; Dondio, G.; Vultaggio, S.; Varasi, M.; Mercurio, C.; Hamel, E.; Lavia, P.; Silvestri, R. New pyrrole derivatives with potent tubulin polymerization inhibiting activity as anticancer agents including Hedgehog-dependent cancer. *J. Med. Chem.* **2014**, *57*, 6531−6552.
(74) Romagnoli, R.; Baraldi, P. G.; Salvador, M. K.; Prencipe, F.; Bertolasi, V.; Cancellieri, M.; Brancale, A.; Hamel, E.; Castagliuolo, I.; Consolaro, F.; Porcù, E.; Basso, G.; Viola, G. Synthesis, antimitotic and antivascular activity of 1-(3′,4′,5′-trimethoxybenzoyl)-3-arylamino-5-amino-1,2,4-triazoles. *J. Med. Chem.* **2014**, *57*, 6795−6808.
(75) León-González, A. J.; Acero, N.; Muñoz-Mingarro, D.; Navarro, I.; Martín-Cordero, C. Chalcones as promising lead compounds on cancer therapy. *Curr. Med. Chem.* **2015**, *22*, 3407−3425.
(76) Ducki, S. Antimitotic chalcones and related compounds as inhibitors of tubulin assembly. *Anti-Cancer Agents Med. Chem.* **2009**, *9*, 336−347.
(77) Ducki, S.; Rennison, D.; Woo, M.; Kendall, A.; Chabert, J. F. D.; McGown, A. T.; Lawrence, N. J. Combretastatin-like chalcones as inhibitors of microtubule polymerization. Part 1: Synthesis and biological evaluation of antivascular activity. *Bioorg. Med. Chem.* **2009**, *17*, 7698−7710.
(78) Zhu, C.; Zuo, Y.; Wang, R.; Liang, B.; Yue, X.; Wen, G.; Shang, N.; Huang, L.; Chen, Y.; Du, J.; Bu, X. Discovery of potent cytotoxic ortho-aryl chalcones as new scaffold targeting tubulin and mitosis with affinity-based fluorescence. *J. Med. Chem.* **2014**, *57*, 6364−6382.
(79) Martel-Frachet, V.; Keramidas, M.; Nurisso, A.; DeBonis, S.; Rome, C.; Coll, J. L.; Boumendjel, A.; Skoufias, D. A.; Ronot, X. IPP51, a chalcone acting as a microtubule inhibitor with in vivo antitumor activity against bladder carcinoma. *Oncotarget* **2015**, *6*, 14669−14686.
(80) Zheng, S.; Zhong, Q.; Mottamal, M.; Zhang, Q.; Zhang, C.; LeMelle, E.; McFerrin, H.; Wang, G. Design, synthesis, and biological evaluation of novel pyridine-bridged analogues of combretastatin-A4 as anticancer agents. *J. Med. Chem.* **2014**, *57*, 3369−3381.
(81) Yoshimatsu, K.; Yamaguchi, A.; Yoshino, H.; Koyanagi, N.; Kitoh, K. Mechanism of action of E7010, an orally active sulfonamide antitumor agent: inhibition of mitosis by binding to the colchicine site of tubulin. *Cancer Res.* **1997**, *57*, 3208−3213.
(82) Hande, K. R.; Hagey, A.; Berlin, J.; Cai, Y.; Meek, K.; Kobayashi, H.; Lockhart, A. C.; Medina, D.; Sosman, J.; Gordon, G. B.; Rothenberg, M. L. The pharmacokinetics and safety of ABT-751, a novel, orally bioavailable sulfonamide antimitotic agent: results of a phase 1 study. *Clin. Cancer Res.* **2006**, *12*, 2834−2840.
(83) Dorléans, A.; Gigant, B.; Ravelli, R. B.; Mailliet, P.; Mikol, V.; Knossow, M. Variations in the colchicine-binding domain provide insight into the structural switch of tubulin. *Proc. Natl. Acad. Sci. U. S. A.* **2009**, *106*, 13775−13779.
(84) Chang, J. Y.; Hsieh, H. P.; Chang, C. Y.; Hsu, K. S.; Chiang, Y. F.; Chen, C. M.; Kuo, C. C.; Liou, J. P. 7-Aroyl-aminoindoline-1-sulfonamides as a novel class of potent antitubulin agents. *J. Med. Chem.* **2006**, *49*, 6656−6659.
(85) Nicholson, B.; Lloyd, G. K.; Miller, B. R.; Palladino, M. A.; Kiso, Y.; Hayashi, Y.; Neuteboom, S. T. C. NPI-2358 is a tubulin-depolymerizing agent: in-vitro evidence for activity as a tumor vascular-disrupting agent. *Anti-Cancer Drugs* **2006**, *17*, 25−31.
(86) Yamazaki, Y.; Sumikura, M.; Hidaka, K.; Yasui, H.; Kiso, Y.; Yakushiji, F.; Hayashi, Y. Anti-microtubule 'plinabulin' chemical probe KPU-244-B3 labeled both α- and β-tubulin. *Bioorg. Med. Chem.* **2010**, *18*, 3169−3174.

DOI: 10.1021/acs.jmedchem.6b00463
J. Med. Chem. 2016, 59, 8685−8711

(87) Yamazaki, Y.; Kido, Y.; Hidaka, K.; Yasui, H.; Kiso, Y.; Yakushiji, F.; Hayashi, Y. Tubulin photoaffinity labeling study with a plinabulin chemical probe possessing a biotin tag at the oxazole. *Bioorg. Med. Chem.* **2011**, *19*, 595−602.
(88) Wang, Y.; Zhang, H.; Gigant, B.; Yu, Y.; Wu, Y.; Chen, X.; Lai, Q.; Yang, Z.; Chen, Q.; Yang, J. Structures of a diverse set of colchicine binding site inhibitors in complex with tubulin provide a rationale for drug discovery. *FEBS J.* **2016**, *283*, 102−111.
(89) Yamazaki, Y.; Tanaka, K.; Nicholson, B.; Deyanat-Yazdi, G.; Potts, B.; Yoshida, T.; Oda, A.; Kitagawa, T.; Orikasa, S.; Kiso, Y.; Yasui, H.; Akamatsu, M.; Chinen, T.; Usui, T.; Shinozaki, Y.; Yakushiji, F.; Miller, B. R.; Neuteboom, S.; Palladino, M.; Kanoh, K.; Lloyd, G. K.; Hayashi, Y. Synthesis and structure−activity relationship study of antimicrotubule agents phenylahistin derivatives with a didehydropiperazine-2,5-dione structure. *J. Med. Chem.* **2012**, *55*, 1056−1071.
(90) Reddy, G. R.; Kuo, C.-C.; Tan, U.-K.; Coumar, M. S.; Chang, C.-Y.; Chiang, Y.-K.; Lai, M.-J.; Yeh, J.-Y.; Wu, S.-Y.; Chang, J.-Y.; Liou, J.-P.; Hsieh, H.-P. Synthesis and structure−activity relationships of 2-amino-1-aroylnaphthalene and 2-hydroxy-1-aroylnaphthalenes as potent antitubulin agents. *J. Med. Chem.* **2008**, *51*, 8163−8167.
(91) Burns, C. J.; Harte, M. F.; Bu, X.; Fantino, E.; Joffe, M.; Sikanyika, H.; Su, S.; Tranberg, C. E.; Wilson, N.; Charman, S. A.; Shackleford, D. M.; Wilks, A. F. Discovery of CYT997: a structurally novel orally active microtubule targeting agent. *Bioorg. Med. Chem. Lett.* **2009**, *19*, 4639−4642.
(92) Burns, C. J.; Fantino, E.; Phillips, I. D.; Su, S.; Harte, M. F.; Bukczynska, P. E.; Frazzetto, M.; Joffe, M.; Kruszelnicki, I.; Wang, B.; Wang, Y.; Wilson, N.; Dilley, R. J.; Wan, S. S.; Charman, S. A.; Shackleford, D. M.; Fida, R.; Malcontenti-Wilson, C.; Wilks, A. F. CYT997: a novel orally active tubulin polymerization inhibitor with potent cytotoxic and vascular disrupting activity in vitro and in vivo. *Mol. Cancer Ther.* **2009**, *8*, 3036−3045.
(93) Bacher, G.; Nickel, B.; Emig, P.; Vanhoefer, U.; Seeber, S.; Shandra, A.; Klenner, T.; Beckers, T. D-24851, a novel synthetic microtubule inhibitor, exerts curative antitumoral activity in vivo, shows efficacy toward multidrug-resistant tumor cells, and lacks neurotoxicity. *Cancer Res.* **2001**, *61*, 392−399.
(94) Oostendorp, R. L.; Witteveen, P. O.; Schwartz, B.; Vainchtein, L. D.; Schot, M.; Nol, A.; Rosing, H.; Beijnen, J. H.; Voest, E. E.; Schellens, J. H. M. Dose-finding and pharmacokinetic study of orally administered indibulin (D-24851) to patients with advanced solid tumors. *Invest. New Drugs* **2010**, *28*, 163−170.
(95) Colley, H. E.; Muthana, M.; Danson, S. J.; Jackson, L. V.; Brett, M. L.; Harrison, J.; Coole, S. F.; Mason, D. P.; Jennings, L. R.; Wong, M.; Tulasi, V.; Norman, D.; Lockey, P. M.; Williams, L.; Dossetter, A. G.; Griffen, E. J.; Thompson, M. J. An orally bioavailable, indole-3-glyoxylamide based series of tubulin polymerization inhibitors showing tumor growth inhibition in a mouse xenograft model of head and neck cancer. *J. Med. Chem.* **2015**, *58*, 9309−9333.
(96) Ricart, A. D.; Ashton, E. A.; Cooney, M. M.; Sarantopoulos, J.; Brell, J. M.; Feldman, M. A.; Ruby, K. E.; Matsuda, K.; Munsey, M. S.; Medina, G.; Zambito, A.; Tolcher, A. W.; Remick, S. C. A phase I study of MN-029 (denibulin), a novel vascular-disrupting agent, in patients with advanced solid tumors. *Cancer Chemother. Pharmacol.* **2011**, *68*, 959−970.
(97) Kasibhatla, S.; Baichwal, V.; Cai, S. X.; Roth, B.; Skvortsova, I.; Skvortsov, S.; Lukas, P.; English, N. M.; Sirisoma, N.; Drewe, J.; Pervin, A.; Tseng, B.; Carlson, R. O.; Pleiman, C. M. MPC-6827: a small-molecule inhibitor of microtubule formation that is not a substrate for multidrug resistance pumps. *Cancer Res.* **2007**, *67*, 5865−5871.
(98) Sirisoma, N.; Pervin, A.; Zhang, H.; Jiang, S.; Willardsen, J. A.; Anderson, M. B.; Mather, G.; Pleiman, C. M.; Kasibhatla, S.; Tseng, B.; Drewe, J.; Cai, S. X. Discovery of N-(4-methoxyphenyl)-N,2-dimethylquinazolin-4-amine, a potent apoptosis inducer and efficacious anticancer agent with high blood brain barrier penetration. *J. Med. Chem.* **2009**, *52*, 2341−2351.
(99) Canela, M. D.; Liekens, S.; Camarasa, M. J.; Priego, E. M.; Pérez-Pérez, M. J. Synthesis and antiproliferative activity of 6-phenylaminopurines. *Eur. J. Med. Chem.* **2014**, *87*, 421−428.
(100) Gangjee, A.; Zhao, Y.; Lin, L.; Raghavan, S.; Roberts, E. G.; Risinger, A. L.; Hamel, E.; Mooberry, S. L. Synthesis and discovery of water-soluble microtubule targeting agents that bind to the colchicine site on tubulin and circumvent Pgp mediated resistance. *J. Med. Chem.* **2010**, *53*, 8116−8128.
(101) Zhang, X.; Raghavan, S.; Ihnat, M.; Thorpe, J. E.; Disch, B. C.; Bastian, A.; Bailey-Downs, L. C.; Dybdal-Hargreaves, N. F.; Rohena, C. C.; Hamel, E.; Mooberry, S. L.; Gangjee, A. The design and discovery of water soluble 4-substituted-2,6-dimethylfuro[2, 3-d]-pyrimidines as multitargeted receptor tyrosine kinase inhibitors and microtubule targeting antitumor agents. *Bioorg. Med. Chem.* **2014**, *22*, 3753−3772.
(102) D'Amato, R. J.; Lin, C. M.; Flynn, E.; Folkman, J.; Hamel, E. 2-Methoxyestradiol, an endogenous mammalian metabolite, inhibits tubulin polymerization by interacting at the colchicine site. *Proc. Natl. Acad. Sci. U. S. A.* **1994**, *91*, 3964−3968.
(103) Leese, M. P.; Leblond, B.; Smith, A.; Newman, S. P.; Di Fiore, A.; De Simone, G.; Supuran, C. T.; Purohit, A.; Reed, M. J.; Potter, B. V. L. 2-Substituted estradiol bis-sulfamates, multitargeted antitumor agents: synthesis, in vitro SAR, protein crystallography, and in vivo activity. *J. Med. Chem.* **2006**, *49*, 7683−7696.
(104) Stengel, C.; Newman, S. P.; Leese, M. P.; Thomas, M. P.; Potter, B. V. L; Reed, M. J.; Purohit, A.; Foster, P. A. The in vitro and in vivo activity of the microtubule disruptor STX140 is mediated by HIF-1 alpha and CAIX expression. *Anticancer Res.* **2015**, *35*, 5249−5262.
(105) Leese, M. P.; Jourdan, F.; Dohle, W.; Kimberley, M. R.; Thomas, M. P.; Bai, R.; Hamel, E.; Ferrandis, E.; Potter, B. V. L. Steroidomimetic tetrahydroisoquinolines for the design of new microtubule disruptors. *ACS Med. Chem. Lett.* **2012**, *3*, 5−9.
(106) Pasquier, E.; Sinnappan, S.; Munoz, M. A.; Kavallaris, M. ENMD-1198, a new analogue of 2-methoxyestradiol, displays both antiangiogenic and vascular-disrupting properties. *Mol. Cancer Ther.* **2010**, *9*, 1408−1418.
(107) Nogales, E.; Wolf, S. G.; Downing, K. H. Structure of the $\alpha\beta$ tubulin dimer by electron crystallography. *Nature* **1998**, *391*, 199−203.
(108) Löwe, J.; Li, H.; Downing, K. H.; Nogales, E. Refined structure of α,β-tubulin at 3.5 Å resolution. *J. Mol. Biol.* **2001**, *313*, 1045−1057.
(109) Janke, C. The tubulin code Molecular components, readout mechanisms, and functions. *J. Cell Biol.* **2014**, *206*, 461−472.
(110) Gigant, B.; Curmi, P. A.; Martin-Barbey, C.; Charbaut, E.; Lachkar, S.; Lebeau, L.; Siavoshian, S.; Sobel, A.; Knossow, M. The 4 Å X-Ray structure of a tubulin:stathmin-like domain complex. *Cell* **2000**, *102*, 809−816.
(111) Barbier, P.; Dorléans, A.; Devred, F.; Sanz, L.; Allegro, D.; Alfonso, C.; Knossow, M.; Peyrot, V.; Andreu, J. M. Stathmin and interfacial microtubule inhibitors recognize a naturally curved conformation of tubulin dimers. *J. Biol. Chem.* **2010**, *285*, 31672−31681.
(112) Arce, C. A.; Rodriguez, J. A.; Barra, H. S.; Caputto, R. Incorporation of L-tyrosine, L-phenylalanine and L-3,4-dihydroxyphenylalanine as single units into rat-brain tubulin. *Eur. J. Biochem.* **1975**, *59*, 145−149.
(113) Prota, A. E.; Magiera, M. M.; Kuijpers, M.; Bargsten, K.; Frey, D.; Wieser, M.; Jaussi, R.; Hoogenraad, C. C.; Kammerer, R. A.; Janke, C.; Steinmetz, M. O. Structural basis of tubulin tyrosination by tubulin tyrosine ligase. *J. Cell Biol.* **2013**, *200*, 259−270.
(114) Prota, A. E.; Bargsten, K.; Zurwerra, D.; Field, J. J.; Diaz, J. F.; Altmann, K.-H.; Steinmetz, M. O. Molecular mechanism of action of microtubule-stabilizing anticancer agents. *Science* **2013**, *339*, 587−590.
(115) Prota, A. E.; Danel, F.; Bachmann, F.; Bargsten, K.; Buey, R. M.; Pohlmann, J.; Reinelt, S.; Lane, H.; Steinmetz, M. O. The novel microtubule-destabilizing drug BAL27862 binds to the colchicine site of tubulin with distinct effects on microtubule organization. *J. Mol. Biol.* **2014**, *426*, 1848−1860.

DOI: 10.1021/acs.jmedchem.6b00463
J. Med. Chem. 2016, 59, 8685−8711

(116) Prota, A. E.; Bargsten, K.; Diaz, J. F.; Marsh, M.; Cuevas, C.; Liniger, M.; Neuhaus, C.; Andreu, J. M.; Altmann, K.-H.; Steinmetz, M. O. A new tubulin-binding site and pharmacophore for microtubule-destabilizing anticancer drugs. *Proc. Natl. Acad. Sci. U. S. A.* **2014**, *111*, 13817−13821.
(117) McNamara, D. E.; Senese, S.; Yeates, T. O.; Torres, J. Z. Structures of potent anticancer compounds bound to tubulin. *Protein Sci.* **2015**, *24*, 1164−1172.
(118) Deng, Z.; Chuaqui, C.; Singh, J. Structural interaction fingerprint (SIFt): a novel method for analyzing three-dimensional protein−ligand binding interactions. *J. Med. Chem.* **2004**, *47*, 337−344.
(119) Pecqueur, L.; Duellberg, C.; Dreier, B.; Jiang, Q.; Wang, C.; Plueckthun, A.; Surrey, T.; Gigant, B.; Knossow, M. A designed ankyrin repeat protein selected to bind to tubulin caps the microtubule plus end. *Proc. Natl. Acad. Sci. U. S. A.* **2012**, *109*, 12011−12016.
(120) Ayaz, P.; Ye, X.; Huddleston, P.; Brautigam, C. A.; Rice, L. M. A TOG:alpha beta-tubulin complex structure reveals conformation-based mechanisms for a microtubule polymerase. *Science* **2012**, *337*, 857−860.
(121) Skoufias, D. A.; Wilson, L. Mechanism of inhibition of microtubule polymerization by colchicine - inhibitory potencies of unliganded colchicine and tubulin colchicine complexes. *Biochemistry* **1992**, *31*, 738−746.
(122) Akhmanova, A.; Steinmetz, M. O. Control of microtubule organization and dynamics: two ends in the limelight. *Nat. Rev. Mol. Cell Biol.* **2015**, *16*, 711−726.
(123) O'Boyle, N. M.; Greene, L. M.; Keely, N. O.; Wang, S.; Cotter, T. S.; Zisterer, D. M.; Meegan, M. J. Synthesis and biochemical activities of antiproliferative amino acid and phosphate derivatives of microtubule-disrupting β-lactam combretastatins. *Eur. J. Med. Chem.* **2013**, *62*, 705−721.
(124) Aprile, S.; Zaninetti, R.; Del Grosso, E.; Genazzani, A. A.; Grosa, G. Metabolic fate of combretastatin A-1: LC-DAD-MS/MS investigation and biological evaluation of its reactive metabolites. *J. Pharm. Biomed. Anal.* **2013**, *78*−*79*, 233−242.
(125) Rautio, J.; Kumpulainen, H.; Heimbach, T.; Oliyai, R.; Oh, D.; Jarvinen, T.; Savolainen, J. Prodrugs: design and clinical applications. *Nat. Rev. Drug Discovery* **2008**, *7*, 255−270.
(126) Eskens, F. A. L. M.; Tresca, P.; Tosi, D.; Van Doorn, L.; Fontaine, H.; Van der Gaast, A.; Veyrat-Follet, C.; Oprea, C.; Hospitel, M.; Dieras, V. A phase I pharmacokinetic study of the vascular disrupting agent ombrabulin (AVE8062) and docetaxel in advanced solid tumours. *Br. J. Cancer* **2014**, *110*, 2170−2177.
(127) Nkepang, G.; Bio, M.; Rajaputra, P.; Awuah, S. G.; You, Y. Folate receptor-mediated enhanced and specific delivery of far-red light-activatable prodrugs of combretastatin A-4 to FR-positive tumor. *Bioconjugate Chem.* **2014**, *25*, 2175−2188.
(128) Yang, T.; Wang, Y.; Li, Z.; Dai, W.; Yin, J.; Liang, L.; Ying, X.; Zhou, S.; Wang, J.; Zhang, X.; Zhang, Q. Targeted delivery of a combination therapy consisting of combretastatin A4 and low-dose doxorubicin against tumor neovasculature. *Nanomedicine* **2012**, *8*, 81−92.
(129) Zhang, Y.; Wang, J.; Bian, D.; Zhang, X.; Zhang, Q. Targeted delivery of RGD-modified liposomes encapsulating both combretastatin A-4 and doxorubicin for tumor therapy: In vitro and in vivo studies. *Eur. J. Pharm. Biopharm.* **2010**, *74*, 467−473.
(130) Zhang, M.; Guo, R.; Wang, Y.; Cao, X.; Shen, M.; Shi, X. Multifunctional dendrimer/combretastatin A4 inclusion complexes enable in vitro targeted cancer therapy. *Int. J. Nanomed.* **2011**, *6*, 2337−2349.
(131) Wang, Y.; Chen, H.; Liu, Y.; Wu, J.; Zhou, P.; Wang, Y.; Li, R.; Yang, X.; Zhang, N. pH-sensitive pullulan-based nanoparticle carrier of methotrexate and combretastatin A4 for the combination therapy against hepatocellular carcinoma. *Biomaterials* **2013**, *34*, 7181−7190.
(132) Sengupta, S.; Eavarone, D.; Capila, I.; Zhao, G.; Watson, N.; Kiziltepe, T.; Sasisekharan, R. Temporal targeting of tumour cells and neovasculature with a nanoscale delivery system. *Nature* **2005**, *436*, 568−572.
(133) Poojari, R.; Kini, S.; Srivastava, R.; Panda, D. A chimeric cetuximab-functionalized corona as a potent delivery system for microtubule-destabilizing nanocomplexes to hepatocellular carcinoma cells: a focus on EGFR and tubulin intracellular dynamics. *Mol. Pharmaceutics* **2015**, *12*, 3908−3923.
(134) Song, W.; Tang, Z.; Zhang, D.; Yu, H.; Chen, X. Coadministration of vascular disrupting agents and nanomedicines to eradicate tumors from peripheral and central regions. *Small* **2015**, *11*, 3755−3761.
(135) Al-Abd, A. M.; Aljehani, Z. K.; Gazzaz, R. W.; Fakhri, S. H.; Jabbad, A. H.; Alahdal, A. M.; Torchilin, V. P. Pharmacokinetic strategies to improve drug penetration and entrapment within solid tumors. *J. Controlled Release* **2015**, *219*, 269−277.
(136) Tozer, G. M.; Prise, V. E.; Wilso, J.; Cemazar, M.; Shan, S.; Dewhirst, M. W.; Barber, P. R.; Vojnovic, B.; Chaplin, D. J. Mechanisms associated with tumor vascular shut-down induced by combretastatin A-4 phosphate: Intravital microscopy and measurement of vascular permeability. *Cancer Res.* **2001**, *61*, 6413−6422.
(137) McPhail, L. D.; Griffiths, J. R.; Robinson, S. P. Assessment of tumor response to the vascular disrupting agents 5,6-dimethylxanthenone-4-acetic acid or combretastatin-A4-phosphate by intrinsic susceptibility magnetic resonance imaging. *Int. J. Radiat. Oncol., Biol., Phys.* **2007**, *69*, 1238−1245.
(138) Chen, G.; Horsman, M. R.; Pedersen, M.; Pang, Q.; Stødkilde-Jørgensen, H. The effect of combretastatin A4 disodium phosphate and 5,6- dimethylxanthenone-4-acetic acid on water diffusion and blood perfusion in tumours. *Acta Oncol.* **2008**, *47*, 1071−1076.
(139) Zhao, D.; Richer, E.; Antich, P. P.; Mason, R. P. Antivascular effects of combretastatin A4 phosphate in breast cancer xenograft assessed using dynamic bioluminescence imaging and confirmed by MRI. *FASEB J.* **2008**, *22*, 2445−2451.
(140) Nielsen, T.; Bentzen, L.; Pedersen, M.; Tramm, T.; Rijken, P. F. J. W.; Bussink, J.; Horsman, M. R.; Ostergaard, L. Combretastatin A-4 phosphate affects tumor vessel volume and size distribution as assessed using MRI-based vessel size imaging. *Clin. Cancer Res.* **2012**, *18*, 6469−6477.
(141) Horsman, M. R.; Murata, R.; Breidahl, T.; Nielsen, F. U.; Maxwell, R. J.; Stødkiled-Jørgensen, H.; Overgaard, J. Combretastatins novel vascular targeting drugs for improving anti-cancer therapy: Combretastatins and conventional therapy. *Adv. Exp. Med. Biol.* **2000**, *476*, 311−323.
(142) Lunt, S. J.; Akerman, S.; Hill, S. A.; Fisher, M.; Wright, V. J.; Reyes-Aldasoro, C. C.; Tozer, G. M.; Kanthou, C. Vascular effects dominate solid tumor response to treatment with combretastatin A-4-phosphate. *Int. J. Cancer* **2011**, *129*, 1979−1989.
(143) Ley, C. D.; Horsman, M. R.; Kristjansen, P. E. G. Early effects of combretastatin-A4 disodium phosphate on tumor perfusion and interstitial fluid pressure. *Neoplasia* **2007**, *9*, 108−112.
(144) Williams, L. J.; Mukherjee, D.; Fisher, M.; Reyes-Aldasoro, C. C.; Akerman, S.; Kanthou, C.; Tozer, G. M. An in vivo role for Rho kinase activation in the tumour vascular disrupting activity of combretastatin A-4 3-O-phosphate. *Br. J. Pharmacol.* **2014**, *171*, 4902−4913.
(145) Vincent, L.; Kermani, P.; Young, L. M.; Cheng, J.; Zhang, F.; Shido, K.; Lam, G.; Bompais-Vincent, H.; Zhu, Z.; Hicklin, D. J.; Bohlen, P.; Chaplin, D. J.; May, C.; Rafii, S. Combretastatin A4 phosphate induces rapid regression of tumor neovessels and growth through interference with vascular endothelial-cadherin signaling. *J. Clin. Invest.* **2005**, *115*, 2992−3006.
(146) Hussain, A.; Steimle, M.; Hoppeler, H.; Baum, O.; Egginton, S. The vascular-disrupting agent combretastatin impairs splitting and sprouting forms of physiological angiogenesis. *Microcirculation* **2012**, *19*, 296−305.
(147) Jiang, Z.; Wu, M.; Miao, J.; Duan, H.; Zhang, S.; Chen, M.; Sun, L.; Wang, Y.; Zhang, X.; Zhu, X.; Zhang, L. Deoxypodophyllotoxin exerts both anti-angiogenic and vascular disrupting effects. *Int. J. Biochem. Cell Biol.* **2013**, *45*, 1710−1719.
(148) Ahmed, B.; Van Eijk, L. I.; Bouma-ter Steege, J. C. A.; Van Der Schaft, D. W. J.; Van Esch, A. M.; Joosten-Achjanie, S. R.; Lambin, P.;

DOI: 10.1021/acs.jmedchem.6b00463
J. Med. Chem. 2016, 59, 8685−8711

Landuyt, W.; Griffioen, A. W. Vascular targeting effect of combretastatin A-4 phosphate dominates the inherent angiogenesis inhibitory activity. *Int. J. Cancer* **2003**, *105*, 20−25.
(149) Porcù, E.; Viola, G.; Bortolozzi, R.; Persano, L.; Mitola, S.; Ronca, R.; Presta, M.; Romagnoli, R.; Baraldi, P. G.; Basso, G. TR-644 a novel potent tubulin binding agent induces impairment of endothelial cells function and inhibits angiogenesis. *Angiogenesis* **2013**, *16*, 647−662.
(150) Samarin, J.; Rehm, M.; Krueger, B.; Waschke, J.; Goppelt-Struebe, M. Up-regulation of connective tissue growth factor in endothelial cells by the microtubule-destabilizing agent combretastatin A-4. *Mol. Cancer Res.* **2009**, *7*, 180−188.
(151) Alotaibi, M. R.; Asnake, B.; Di, X.; Beckman, M. J.; Durrant, D.; Simoni, D.; Baruchello, R.; Lee, R. M.; Schwartz, E. L.; Gewirtz, D. A. Stilbene 5c, a microtubule poison with vascular disrupting properties that induces multiple modes of growth arrest and cell death. *Biochem. Pharmacol.* **2013**, *86*, 1688−1698.
(152) Shen, C. H.; Shee, J. J.; Wu, J. Y.; Lin, Y. W.; Wu, J. D.; Liu, Y. W. Combretastatin A-4 inhibits cell growth and metastasis in bladder cancer cells and retards tumour growth in a murine orthotopic bladder tumour model. *Br. J. Pharmacol.* **2010**, *160*, 2008−2027.
(153) Kanthou, C.; Greco, O.; Stratford, A.; Cook, I.; Knight, R.; Benzakour, O.; Tozer, G. The tubulin-binding agent combretastatin A-4-phosphate arrests endothelial cells in mitosis and induces mitotic cell death. *Am. J. Pathol.* **2004**, *165*, 1401−1411.
(154) Nabha, S. M.; Mohammad, R. M.; Dandashi, M. H.; Coupaye-Gerard, B.; Aboukameel, A.; Pettit, G. R.; Al-Katib, A. M. Combretastatin-A4 prodrug induces mitotic catastrophe in chronic lymphocytic leukemia cell line independent of caspase activation and poly(ADP-ribose) polymerase cleavage. *Clin. Cancer Res.* **2002**, *8*, 2735−2741.
(155) Vitale, I.; Galluzzi, L.; Castedo, M.; Kroemer, G. Mitotic catastrophe: a mechanism for avoiding genomic instability. *Nat. Rev. Mol. Cell Biol.* **2011**, *12*, 385−392.
(156) Nabha, S. M.; Wall, N. R.; Mohammad, R. M.; Pettit, G. R.; Al-Katib, A. M. Effects of Combretastatin A-4 prodrug against a panel of malignant human B-lymphoid cell lines. *Anti-Cancer Drugs* **2000**, *11*, 385−392.
(157) Cenciarelli, C.; Tanzarella, C.; Vitale, I.; Pisano, C.; Crateri, P.; Meschini, S.; Arancia, G.; Antoccia, A. The tubulin-depolymerising agent combretastatin-4 induces ectopic aster assembly and mitotic catastrophe in lung cancer cells H460. *Apoptosis* **2008**, *13*, 659−669.
(158) Vitale, I.; Antoccia, A.; Cenciarelli, C.; Crateri, P.; Meschini, S.; Arancia, G.; Pisano, C.; Tanzarella, C. Combretastatin CA-4 and combretastatin derivative induce mitotic catastrophe dependent on spindle checkpoint and caspase-3 activation in non-small cell lung cancer cells. *Apoptosis* **2007**, *12*, 155−166.
(159) O'Boyle, N. M.; Carr, M.; Greene, L. M.; Keely, N. O.; Knox, A. J. S.; McCabe, T.; Lloyd, D. G.; Zisterer, D. M.; Meegan, M. J. Synthesis, biochemical and molecular modelling studies of anti-proliferative azetidinones causing microtubule disruption and mitotic catastrophe. *Eur. J. Med. Chem.* **2011**, *46*, 4595−4607.
(160) Green, D. R.; Llambi, F. Cell death signaling. *Cold Spring Harbor Perspect. Biol.* **2015**, *7*, a006080.
(161) Iyer, S.; Chaplin, D. J.; Rosenthal, D. S.; Boulares, A. H.; Li, L. Y.; Smulson, M. E. Induction of apoptosis in proliferating human endothelial cells by the tumor-specific antiangiogenesis agent combretastatin A-4. *Cancer Res.* **1998**, *58*, 4510−4514.
(162) Petit, I.; Karajannis, M. A.; Vincent, L.; Young, L.; Butler, J.; Hooper, A. T.; Shido, K.; Steller, H.; Chaplin, D. J.; Feldman, E.; Rafii, S. The microtubule-targeting agent CA4P regresses leukemic xenografts by disrupting interaction with vascular cells and mitochondrial-dependent cell death. *Blood* **2008**, *111*, 1951−1961.
(163) Mendez, G.; Policarpi, C.; Cenciarelli, C.; Tanzarella, C.; Antoccia, A. Role of Bim in apoptosis induced in H460 lung tumor cells by the spindle poison combretastatin-A4. *Apoptosis* **2011**, *16*, 940−949.
(164) Méndez-Callejas, G. M.; Leone, S.; Tanzarella, C.; Antoccia, A. Combretastatin A-4 induces p53 mitochondrial-relocalisation independent-apoptosis in non-small lung cancer cells. *Cell Biol. Int.* **2014**, *38*, 296−308.
(165) Mahal, K.; Ahmad, A.; Sethi, S.; Resch, M.; Ficner, R.; Sarkar, F. H.; Schobert, R.; Biersack, B. Role of JNK and NF-κB in mediating the effect of combretastatin A-4 and brimamin on endothelial and carcinoma cells. *Cell. Oncol.* **2015**, *38*, 463−478.
(166) Lin, H. L.; Chiou, S. H.; Wu, C. W.; Lin, W. B.; Chen, L. H.; Yang, Y. P.; Tsai, M. L.; Uen, Y. H.; Liou, J. P.; Chi, C. W. Combretastatin A4-induced differential cytotoxicity and reduced metastatic ability by inhibition of AKT function in human gastric cancer cells. *J. Pharmacol. Exp. Ther.* **2007**, *323*, 365−373.
(167) Pollock, J. K.; Verma, N. K.; O'Boyle, N. M.; Carr, M.; Meegan, M. J.; Zisterer, D. M. Combretastatin (CA)-4 and its novel analogue CA-432 impair T-cell migration through the Rho/ROCK signalling pathway. *Biochem. Pharmacol.* **2014**, *92*, 544−557.
(168) Hori, K.; Saito, S.; Kubota, K. A novel combretastatin A-4 derivative, AC7700, strongly stanches tumour blood flow and inhibits growth of tumours developing in various tissues and organs. *Br. J. Cancer* **2002**, *86*, 1604−1614.
(169) Ridley, A. J. Rho GTPase signalling in cell migration. *Curr. Opin. Cell Biol.* **2015**, *36*, 103−112.
(170) Kanthou, C.; Tozer, G. M. The tumor vascular targeting agent combretastatin A-4-phosphate induces reorganization of the actin cytoskeleton and early membrane blebbing in human endothelial cells. *Blood* **2002**, *99*, 2060−2069.
(171) Wang, Y.; Wang, B.; Guerram, M.; Sun, L.; Shi, W.; Tian, C.; Zhu, X.; Jiang, Z.; Zhang, L. Deoxypodophyllotoxin suppresses tumor vasculature in HUVECs by promoting cytoskeleton remodeling through LKB1-AMPK dependent Rho A activation. *Oncotarget* **2015**, *6*, 29497−29512.
(172) Hori, K.; Akita, H.; Nonaka, H.; Sumiyoshi, A.; Taki, Y. Prevention of cancer recurrence in tumor margins by stopping microcirculation in the tumor and tumor-host interface. *Cancer Sci.* **2014**, *105*, 1196−1204.
(173) Yao, N.; Ren, K.; Jiang, C.; Gao, M.; Huang, D.; Lu, X.; Lou, B.; Peng, F.; Yang, A.; Wang, X.; Ni, Y.; Zhang, J. Combretastatin A4 phosphate treatment induces vasculogenic mimicry formation of W256 breast carcinoma tumor in vitro and in vivo. *Tumor Biol.* **2015**, *36*, 8499−8510.
(174) El-Emir, E.; Boxer, G. M.; Petrie, I. A.; Boden, R. W.; Dearling, J. L. J.; Begent, R. H. J.; Pedley, R. B. Tumour parameters affected by combretastatin A-4 phosphate therapy in a human colorectal xenograft model in nude mice. *Eur. J. Cancer* **2005**, *41*, 799−806.
(175) Dachs, G. U.; Steele, A. J.; Coralli, C.; Kanthou, C.; Brooks, A. C.; Gunningham, S. P.; Currie, M. J.; Watson, A. I.; Robinson, B. A.; Tozer, G. M. Anti-vascular agent Combretastatin A-4-P modulates hypoxia inducible factor-1 and gene expression. *BMC Cancer* **2006**, *6*, 280.
(176) Peichev, M.; Naiyer, A. J.; Pereira, D.; Zhu, Z.; Lane, W. J.; Williams, M.; Oz, M. C.; Hicklin, D. J.; Witte, L.; Moore, M. A. S.; Rafii, S. Expression of VEGFR-2 and AC133 by circulating human CD34+ cells identifies a population of functional endothelial precursors. *Blood* **2000**, *95*, 952−958.
(177) Nolan, D. J.; Ciarrocchi, A.; Mellick, A. S.; Jaggi, J. S.; Bambino, K.; Gupta, S.; Heikamp, E.; McDevitt, M. R.; Scheinberg, D. A.; Benezra, R.; Mittal, V. Bone marrow-derived endothelial progenitor cells are a major determinant of nascent tumor neovascularization. *Genes Dev.* **2007**, *21*, 1546−1558.
(178) Ceradini, D. J.; Kulkarni, A. R.; Callaghan, M. J.; Tepper, O. M.; Bastidas, N.; Kleinman, M. E.; Capla, J. M.; Galiano, R. D.; Levine, J. P.; Gurtner, G. C. Progenitor cell trafficking is regulated by hypoxic gradients through HIF-1 induction of SDF-1. *Nat. Med.* **2004**, *10*, 858−864.
(179) Moschetta, M.; Mishima, Y.; Sahin, I.; Manier, S.; Glavey, S.; Vacca, A.; Roccaro, A. M.; Ghobrial, I. M. Role of endothelial progenitor cells in cancer progression. *Biochim. Biophys. Acta, Rev. Cancer* **2014**, *1846*, 26−39.
(180) Shaked, Y.; Tang, T.; Woloszynek, J.; Daenen, L. G.; Man, S.; Xu, P.; Cai, S. R.; Arbeit, J. M.; Voest, E. E.; Chaplin, D. J.; Smythe, J.;

DOI: 10.1021/acs.jmedchem.6b00463
J. Med. Chem. 2016, 59, 8685−8711

Harris, A.; Nathan, P.; Judson, I.; Rustin, G.; Bertolini, F.; Link, D. C.; Kerbel, R. S. Contribution of granulocyte colony-stimulating factor to the acute mobilization of endothelial precursor cells by vascular disrupting agents. *Cancer Res.* **2009**, *69*, 7524−7528.
(181) Shaked, Y.; Ciarrocchi, A.; Franco, M.; Lee, C. R.; Man, S.; Cheung, A. M.; Hicklin, D. J.; Chaplin, D.; Foster, F. S.; Benezra, R.; Kerbel, R. S. Therapy-induced acute recruitment of circulating endothelial progenitor cells to tumors. *Science* **2006**, *313*, 1785−1787.
(182) Lewis, C. E.; De Palma, M.; Naldini, L. Tie2-expressing monocytes and tumor angiogenesis: Regulation by hypoxia and angiopoietin-2. *Cancer Res.* **2007**, *67*, 8429−8432.
(183) Welford, A. F.; Biziato, D.; Coffelt, S. B.; Nucera, S.; Fisher, M.; Pucci, F.; Di Serio, C.; Naldini, L.; De Palma, M.; Tozer, G. M.; Lewis, C. E. TIE2-expressing macrophages limit the therapeutic efficacy of the vascular-disrupting agent combretastatin A4 phosphate in mice. *J. Clin. Invest.* **2011**, *121*, 1969−1973.
(184) Parkins, C. S.; Holder, A. L.; Hill, S. A.; Chaplin, D. J.; Tozer, G. M. Determinants of anti-vascular action by combretastatin A-4 phosphate: Role of nitric oxide. *Br. J. Cancer* **2000**, *83*, 811−816.
(185) Bohn, A. B.; Wittenborn, T.; Brems-Eskildsen, A. S.; Laurberg, T.; Bertelsen, L. B.; Nielsen, T.; Stødkilde-Jørgensen, H.; Møller, B. K.; Horsman, M. R. A combretastatin-mediated decrease in neutrophil concentration in peripheral blood and the impact on the anti-tumor activity of this drug in two different murine tumor models. *PLoS One* **2014**, *9*, e110091.
(186) Greene, L. M.; O'Boyle, N. M.; Nolan, D. P.; Meegan, M. J.; Zisterer, D. M. The vascular targeting agent Combretastatin-A4 directly induces autophagy in adenocarcinoma-derived colon cancer cells. *Biochem. Pharmacol.* **2012**, *84*, 612−624.
(187) Li, Y.; Luo, P.; Wang, J.; Dai, J.; Yang, X.; Wu, H.; Yang, B.; He, Q. Autophagy blockade sensitizes the anticancer activity of CA-4 via JNK-Bcl-2 pathway. *Toxicol. Appl. Pharmacol.* **2014**, *274*, 319−327.
(188) Clémenson, C.; Jouannot, E.; Merino-Trigo, A.; Rubin-Carrez, C.; Deutsch, E. The vascular disrupting agent ombrabulin (AVE8062) enhances the efficacy of standard therapies in head and neck squamous cell carcinoma xenograft models. *Invest. New Drugs* **2013**, *31*, 273−284.
(189) Martinelli, M.; Bonezzi, K.; Riccardi, E.; Kuhn, E.; Frapolli, R.; Zucchetti, M.; Ryan, A. J.; Taraboletti, G.; Giavazzi, R. Sequence dependent antitumour efficacy of the vascular disrupting agent ZD6126 in combination with paclitaxel. *Br. J. Cancer* **2007**, *97*, 888−894.
(190) Wu, X. Y.; Ma, W.; Gurung, K.; Guo, C. H. Mechanisms of tumor resistance to small-molecule vascular disrupting agents: Treatment and rationale of combination therapy. *J. Formosan Med. Assoc.* **2013**, *112*, 115−124.
(191) Nathan, P.; Zweifel, M.; Padhani, A. R.; Koh, D. M.; Ng, M.; Collins, D. J.; Harris, A.; Carden, C.; Smythe, J.; Fisher, N.; Taylor, N. J.; Stirling, J. J.; Lu, S. P.; Leach, M. O.; Rustin, G. J. S.; Judson, I. Phase I trial of combretastatin A4 phosphate (CA4P) in combination with bevacizumab in patients with advanced cancer. *Clin. Cancer Res.* **2012**, *18*, 3428−3439.
(192) Moens, S.; Goveia, J.; Stapor, P. C.; Cantelmo, A. R.; Carmeliet, P. The multifaceted activity of VEGF in angiogenesis - Implications for therapy responses. *Cytokine Growth Factor Rev.* **2014**, *25*, 473−482.
(193) Lambrechts, D.; Lenz, H. J.; De Haas, S.; Carmeliet, P.; Scherer, S. J. Markers of response for the antiangiogenic agent bevacizumab. *J. Clin. Oncol.* **2013**, *31*, 1219−1230.
(194) Zweifel, M.; Jayson, G. C.; Reed, N. S.; Osborne, R.; Hassan, B.; Ledermann, J.; Shreeves, G.; Poupard, L.; Lu, S. P.; Balkissoon, J.; Chaplin, D. J.; Rustin, G. J. S. Phase II trial of combretastatin A4 phosphate, carboplatin, and paclitaxel in patients with platinum-resistant ovarian cancer. *Ann. Oncol.* **2011**, *22*, 2036−2041.
(195) Sosa, J. A.; Balkissoon, J.; Lu, S. P.; Langecker, P.; Elisei, R.; Jarzab, B.; Bal, C. S.; Marur, S.; Gramza, A.; Ondrey, F. Thyroidectomy followed by fosbretabulin (CA4P) combination regimen appears to suggest improvement in patient survival in anaplastic thyroid cancer. *Surgery* **2012**, *152*, 1078−1087.
(196) von Pawel, J.; Gorbounova, V.; Reck, M.; Kowalski, D. M.; Allard, A.; Chadjaa, M.; Rey, A.; Bennouna, J.; Grossi, F. DISRUPT: A randomised phase 2 trial of ombrabulin (AVE8062) plus a taxane-platinum regimen as first-line therapy for metastatic non-small cell lung cancer. *Lung Cancer* **2014**, *85*, 224−229.
(197) Siemann, D. W.; Mercer, E.; Lepler, S.; Rojiani, A. M. Vascular targeting agents enhance chemotherapeutic agent activities in solid tumor therapy. *Int. J. Cancer* **2002**, *99*, 1−6.
(198) Bilenker, J. H.; Flaherty, K. T.; Rosen, M.; Davis, L.; Gallagher, M.; Stevenson, J. P.; Sun, W.; Vaughn, D.; Giantonio, B.; Zimmer, R.; Schnall, M.; O'Dwyer, P. J. Phase I trial of combretastatin A-4 phosphate with carboplatin. *Clin. Cancer Res.* **2005**, *11*, 1527−1533.
(199) Brouhard, G. J.; Rice, L. M. The contribution of $\alpha\beta$-tubulin curvature to microtubule dynamics. *J. Cell Biol.* **2014**, *207*, 323−334.
(200) Tozer, G. M.; Prise, V. E.; Wilson, J.; Locke, R. J.; Vojnovic, B.; Stratford, M. R. L.; Dennis, M. F.; Chaplin, D. J. Combretastatin A-4 phosphate as a tumor vascular-targeting agent: Early effects in tumors and normal tissues. *Cancer Res.* **1999**, *59*, 1626−1634.
(201) Kim, C.; Yang, H.; Fukushima, Y.; Saw, P.; Lee, J.; Park, J. S.; Park, I.; Jung, J.; Kataoka, H.; Lee, D.; DoHeo, W.; Kim, I.; Jon, S.; Adams, R. H.; Nishikawa, S. I.; Uemura, A.; Koh, G. Vascular RhoJ is an effective and selective target for tumor angiogenesis and vascular disruption. *Cancer Cell* **2014**, *25*, 102−117.
(202) Quan, H.; Xu, Y.; Lou, L. p38 MAPK, but not ERK1/2, is critically involved in the cytotoxicity of the novel vascular disrupting agent combretastatin A4. *Int. J. Cancer* **2008**, *122*, 1730−1737.
(203) Kwon, E. J.; Lo, J. H.; Bhatia, S. N. Smart nanosystems: Bio-inspired technologies that interact with the host environment. *Proc. Natl. Acad. Sci. U. S. A.* **2015**, *112*, 14460−14466.
(204) Lin, K. Y.; Kwon, E. J.; Lo, J. H.; Bhatia, S. N. Drug-induced amplification of nanoparticle targeting to tumors. *Nano Today* **2014**, *9*, 550−559.

DOI: 10.1021/acs.jmedchem.6b00463
J. Med. Chem. 2016, 59, 8685−8711